Non-perturbative effects on the q_T spectrum of the Z

Valerio Bertone
IRFU, CEA, Université Paris-Saclay

April 8, 2025, Standard Model at the LHC, Durham

Drell-Yan production

- Inclusive production of a lepton pair in *pp* collisions:

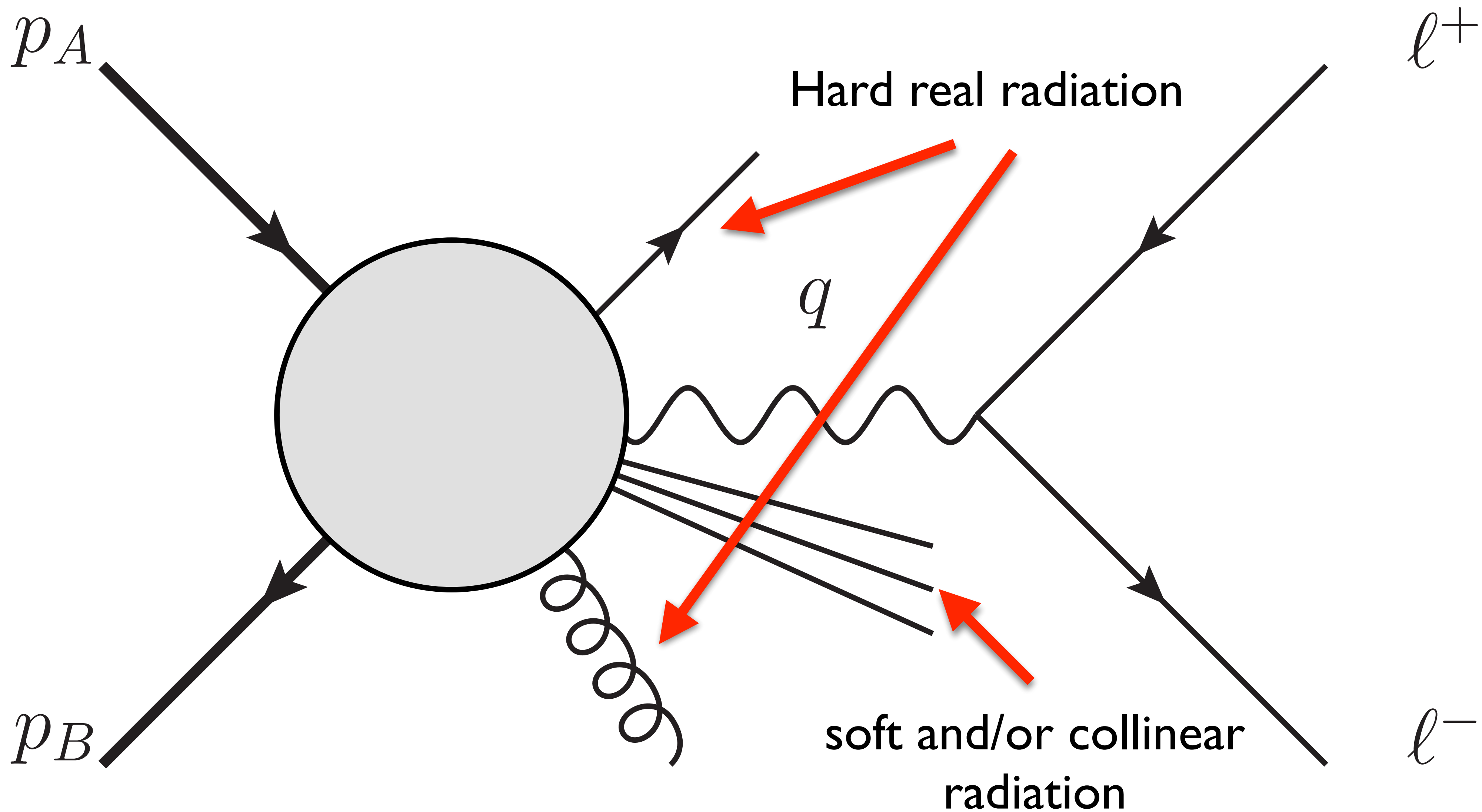

- Relevant scales:

$$Q = \sqrt{q^2}\,, \qquad q_T\,, \qquad Q \gg \Lambda_{\text{QCD}}$$

Resummation formalisms

- Different formulations of the q_T spectrum valid for $q_T \ll Q$ and $q_T \gg \Lambda_{\rm QCD}$:

$$\left(\frac{d\sigma}{dq_T}\right)_{\rm res.} \propto \begin{cases} e^{2S}\left[f_1 \otimes \mathcal{H} \otimes f_2\right] & : q_T \text{ resum.} \\ H \times B_1 \times B_2 \times S & : \text{SCET} \\ H \times F_1 \times F_2 & : \text{TMD} \end{cases} + \mathcal{O}\left[\left(\frac{\Lambda_{\rm QCD}}{q_T}\right)^n, \left(\frac{q_T}{Q}\right)^m\right]$$

- All of them **resum** large $\ln(q_T/Q)$.

- All **equivalent** for *factorising* processes (such as inclusive Drell-Yan).

- Dictionary:

$$\mathcal{H} = H C_1 C_2$$

f_i : Collinear PDFs

$$F_i = e^S C_i \otimes f_i$$

F_i : TMD PDFs

$$F_i = \sqrt{S} \times B_i$$

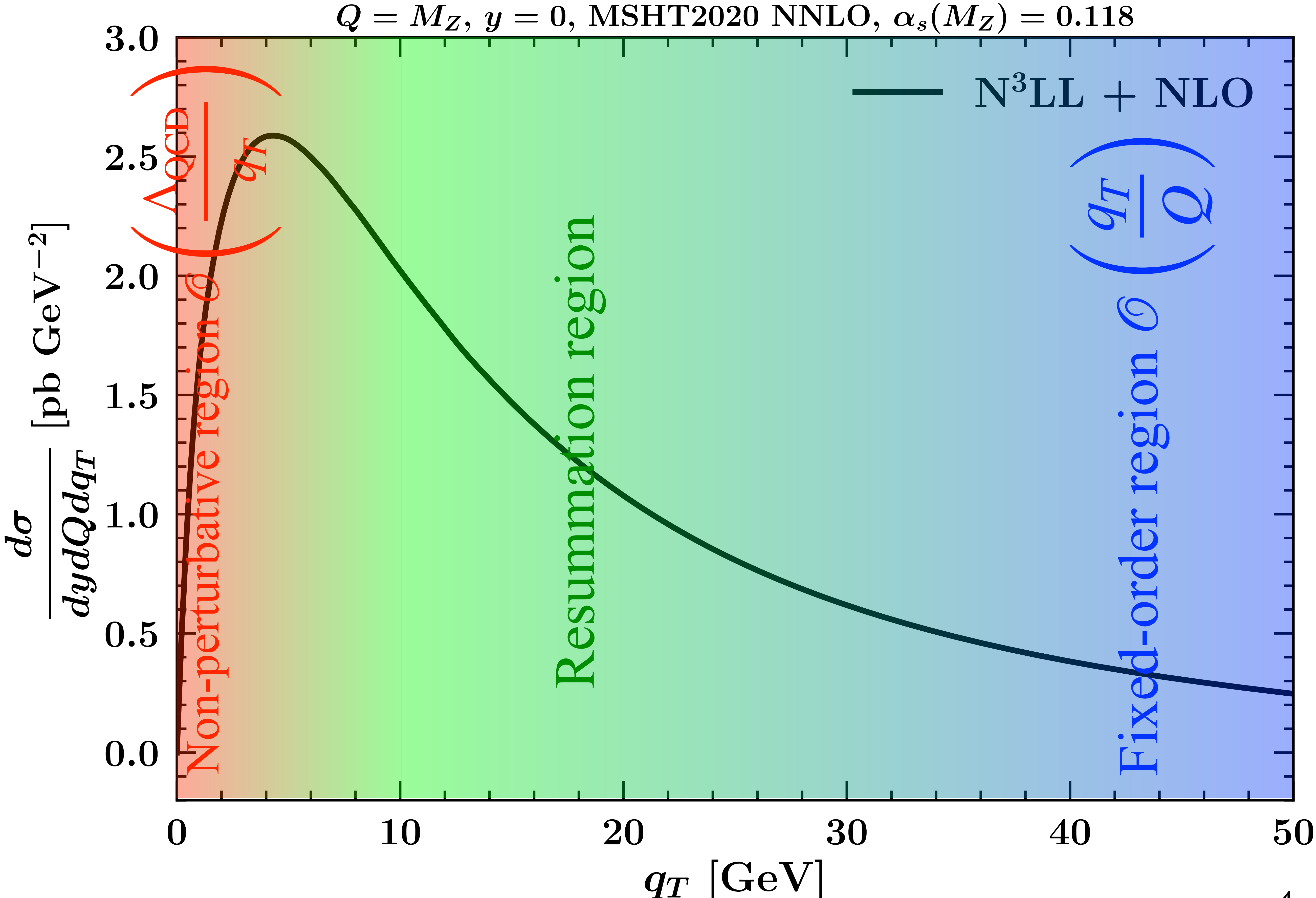

$Q = M_Z,\ y = 0$, MSHT2020 NNLO, $\alpha_s(M_Z) = 0.118$
$\mathbf{N^3LL + NLO}$
Non-perturbative region $\mathcal{O}\left(\frac{\Lambda_{\rm QCD}}{q_T}\right)$
Resummation region
Fixed-order region $\mathcal{O}\left(\frac{q_T}{Q}\right)$
$\frac{d\sigma}{dy\,dQ\,dq_T}$ [pb GeV^{-2}]
q_T [GeV]
0.0
0.5
1.0
1.5
2.0
2.5
3.0
0
10
20
30
40
50

Including $\mathcal{O}(q_T/Q)$ corrections

- Accurate predictions for all $q_T \gg \Lambda_{\rm QCD}$ can be obtained by **matching**:
    - different **recipes** for the matching exist.

$$\left(\frac{d\sigma}{dq_T}\right)_{\rm match.} = \left(\frac{d\sigma}{dq_T}\right)_{\rm res.} + \left(\frac{d\sigma}{dq_T}\right)_{\rm f.o.} - \left(\frac{d\sigma}{dq_T}\right)_{\rm d.c.}$$

- In order for the matching to actually take place one needs:

$$\left(\frac{d\sigma}{dq_T}\right)_{\rm res.} \xrightarrow[\rm f.o.]{} \left(\frac{d\sigma}{dq_T}\right)_{\rm d.c.} \xleftarrow[q_T \ll Q]{} \left(\frac{d\sigma}{dq_T}\right)_{\rm f.o.}$$

- Fixed-order and double-counting terms obey **collinear factorisation**:

$$\left(\frac{d\sigma}{dq_T}\right)_{\rm f.o./d.c} = \int_0^1 dx_1 \int_0^1 dx_2 f_1(x_1, Q) f_2(x_2, Q) \left(\frac{d\hat{\sigma}}{dq_T}\right)_{\rm f.o./d.c}$$

Origin of $\mathcal{O}(\Lambda_{\mathrm{QCD}}/q_T)$ corrections

soft and/or collinear radiation $\Rightarrow \quad \sigma \propto \int_0^Q dk_T\, \alpha_s^p(k_T)\ldots$

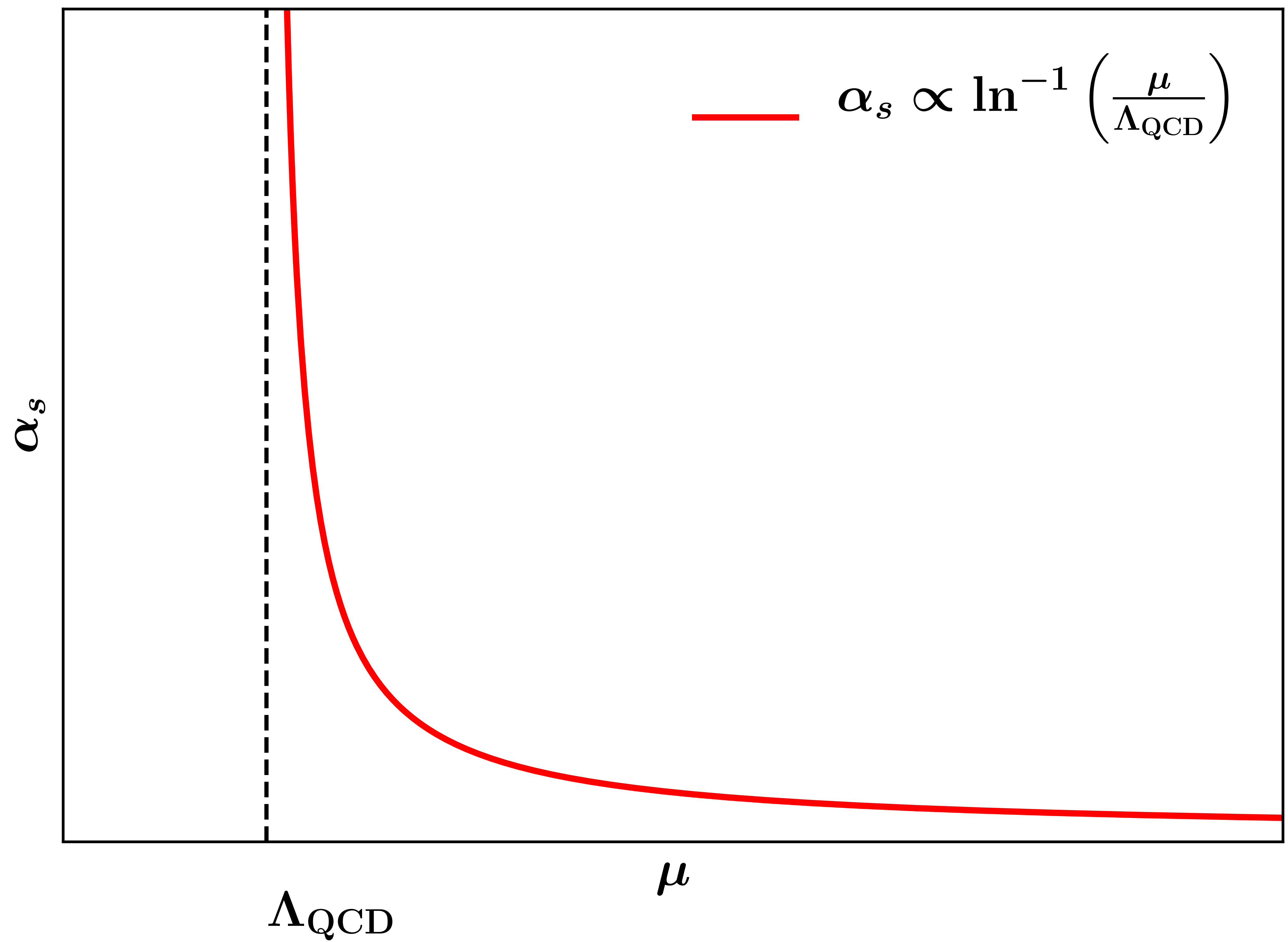

Origin of $\mathcal{O}(\Lambda_{\mathrm{QCD}}/q_T)$ corrections

- **Prescriptions** to avoid integrating over the **Landau pole** introduce power corrections $\mathcal{O}(\Lambda_{\mathrm{QCD}}/q_T)$ of **non-perturbative origin**.
  - different prescriptions distribute these corrections differently.
- To see this, one can use a **dispersive** approach [Bogolyubov, Shirkov; Dokshitzer, Marchesini, Webber]:

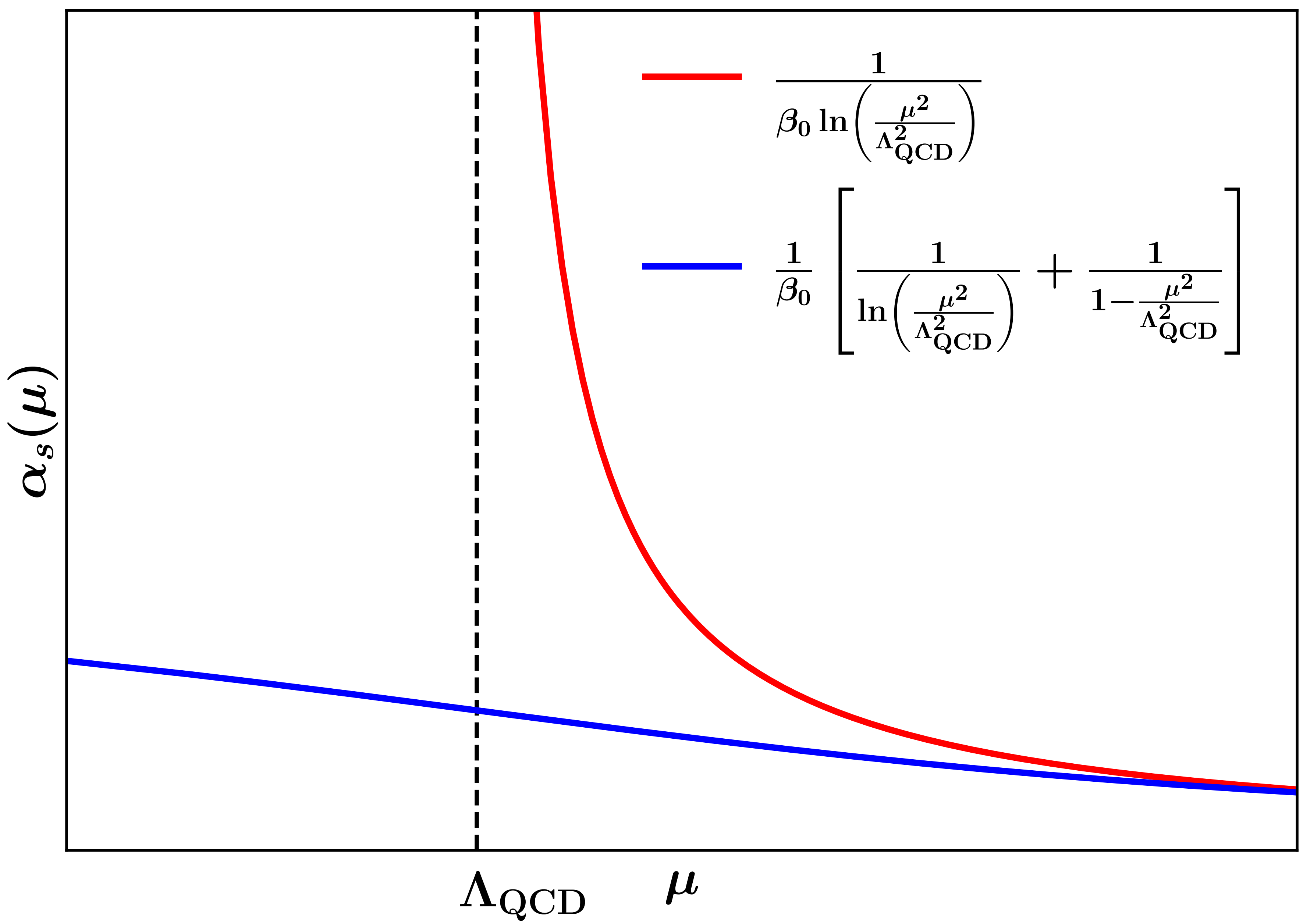

Origin of $\mathcal{O}(\Lambda_{\rm QCD}/q_T)$ corrections

- In the context of the resummation of logs of q_T, dispersive approaches have never been (seriously) considered.
- More popular approaches to the ***regularisation*** of the Landau pole are:

1) The **cutoff** method that leads to corrections that scale as $(\Lambda_{\rm QCD}/q_T)^\alpha$.

In *direct space* (k_T) it amounts to:

$$\alpha_s\,(k_{\rm T}) \to \alpha_s\,(\max[k_{\rm T,cutoff}\,,k_{\rm T}])\;, \qquad k_{\rm T,cutoff} \gg \Lambda_{\rm QCD}$$

In *impact-parameter space* (b_T) it is typically implemented by means of the so-called **b*-prescription**:

$$\alpha_s\left(\frac{2e^{-\gamma_{\rm E}}}{b_{\rm T}}\right) \to \alpha_s\left(\frac{2e^{-\gamma_{\rm E}}}{b_*(b_{\rm T})}\right)$$

A classical choice is:

$$b_*(b_{\rm T}) = \frac{b_{\rm T}}{\sqrt{1+b_{\rm T}^2/b_{\rm max}^2}}$$

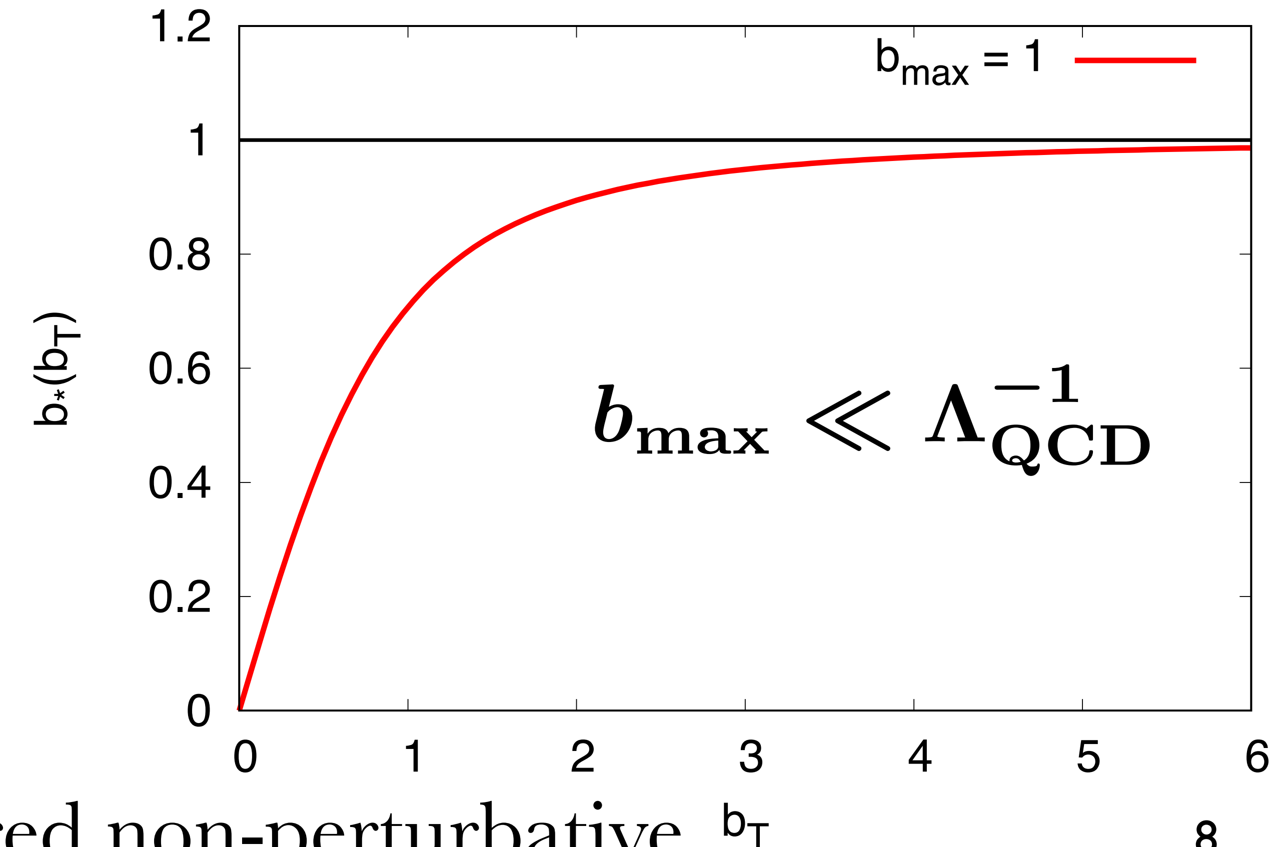

Scales below $b_{\rm max}^{-1} \sim k_{T,\rm cutoff}$ are considered non-perturbative.

Origin of $\mathcal{O}(\Lambda_{\mathrm{QCD}}/q_T)$ corrections

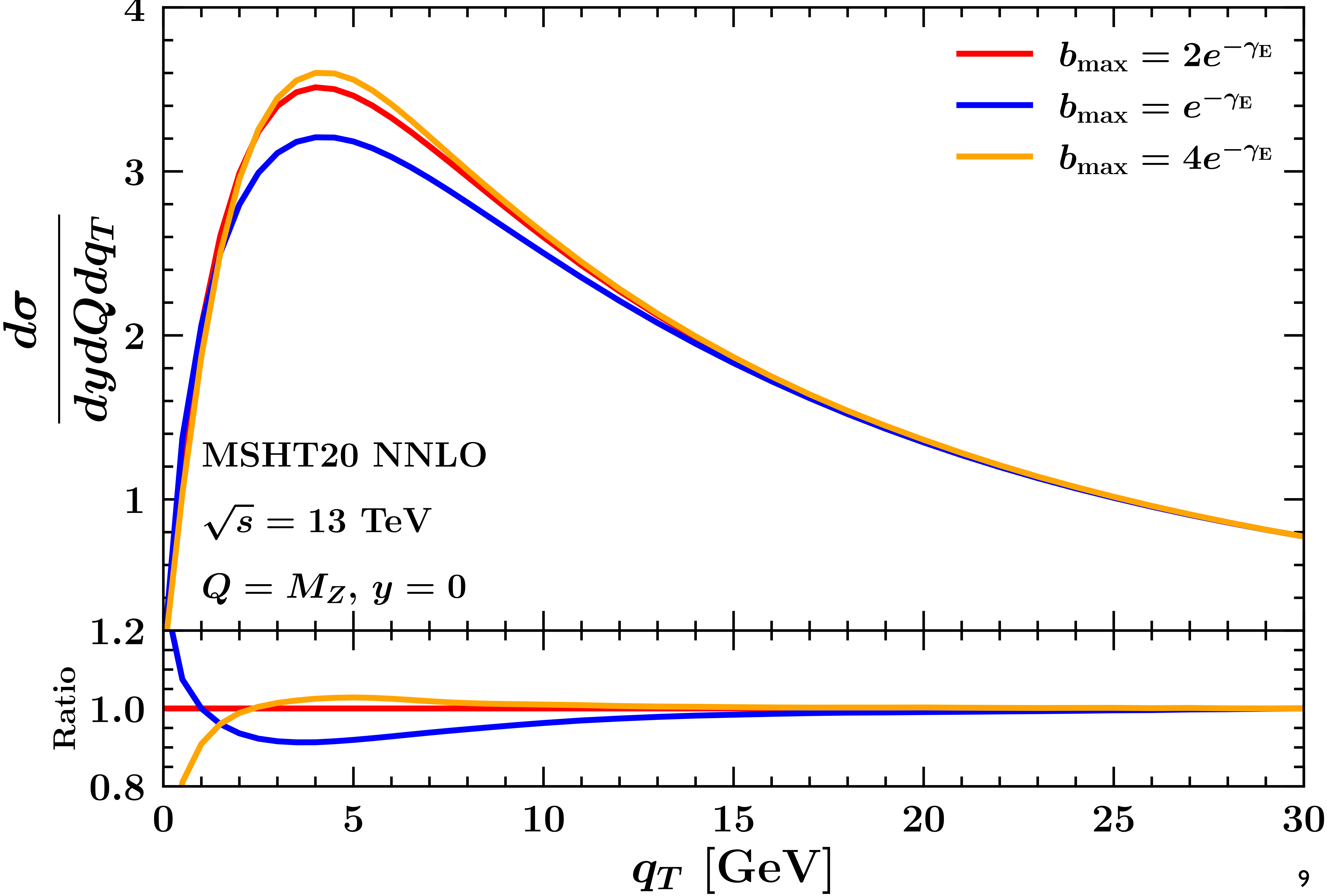

Origin of $\mathcal{O}(\Lambda_{\rm QCD}/q_T)$ corrections

2) The **Minimal Prescription** [Catani, Mangano, Nason, Trentadue]:

$$\int_0^Q dk_{\rm T}\, \alpha_s^p\,(k_{\rm T}) \cdots \to \int_{\frac{\mathcal{C}+\mathcal{C}^*}{2}} dk_{\rm T}\, \alpha_s^p\,(k_{\rm T}) \dots$$

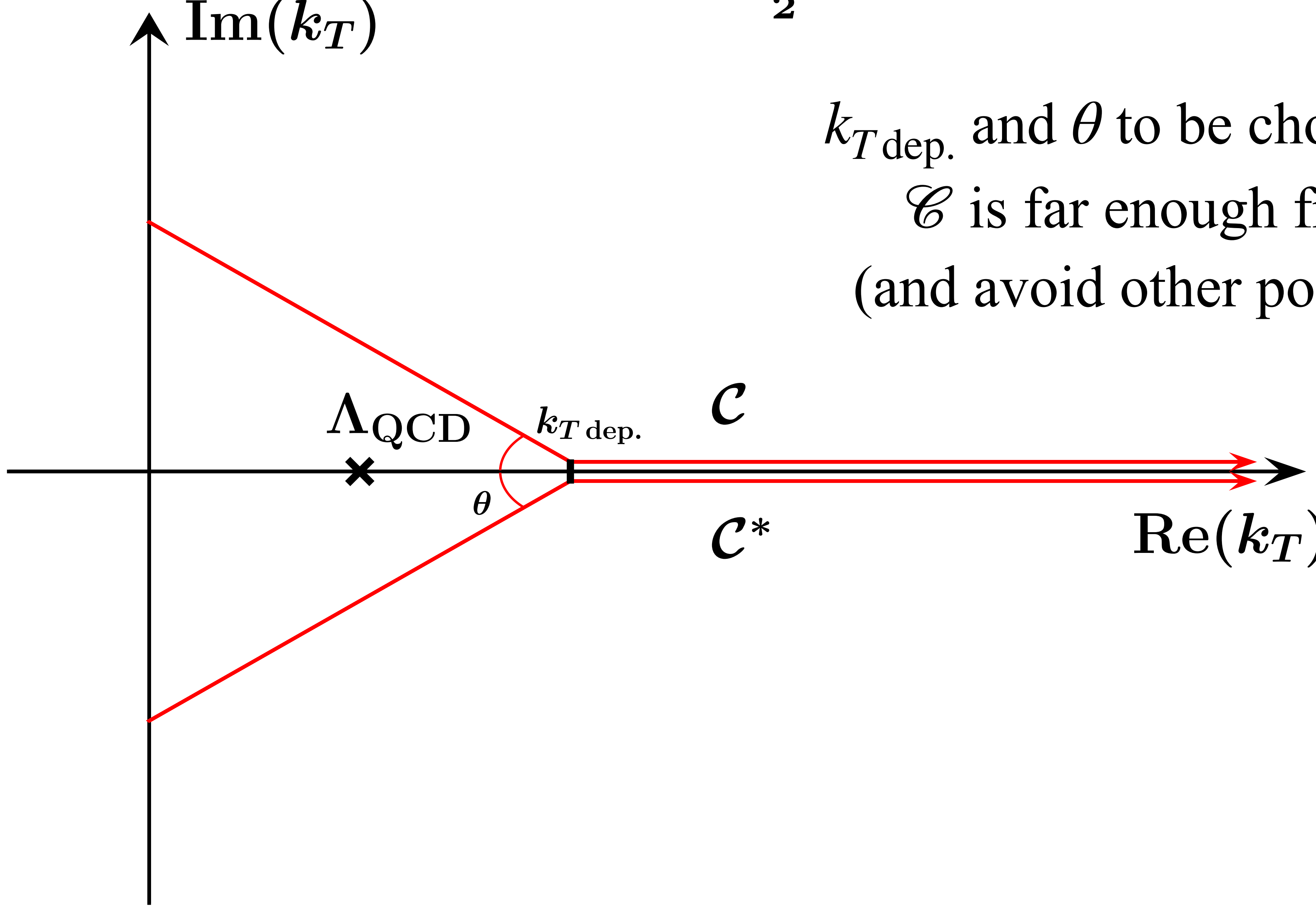

$k_{T\,\rm dep.}$ and θ to be chosen such that $\mathscr{C}$ is far enough from $\Lambda_{\rm QCD}$ (and avoid other possible poles)

The advantage of the MP is that non-perturbative corrections scale as $\exp[-\beta q_T/\Lambda_{\rm QCD}]$, relegating them to smaller values of q_T.

Origin of $\mathcal{O}(\Lambda_{\mathrm{QCD}}/q_T)$ corrections

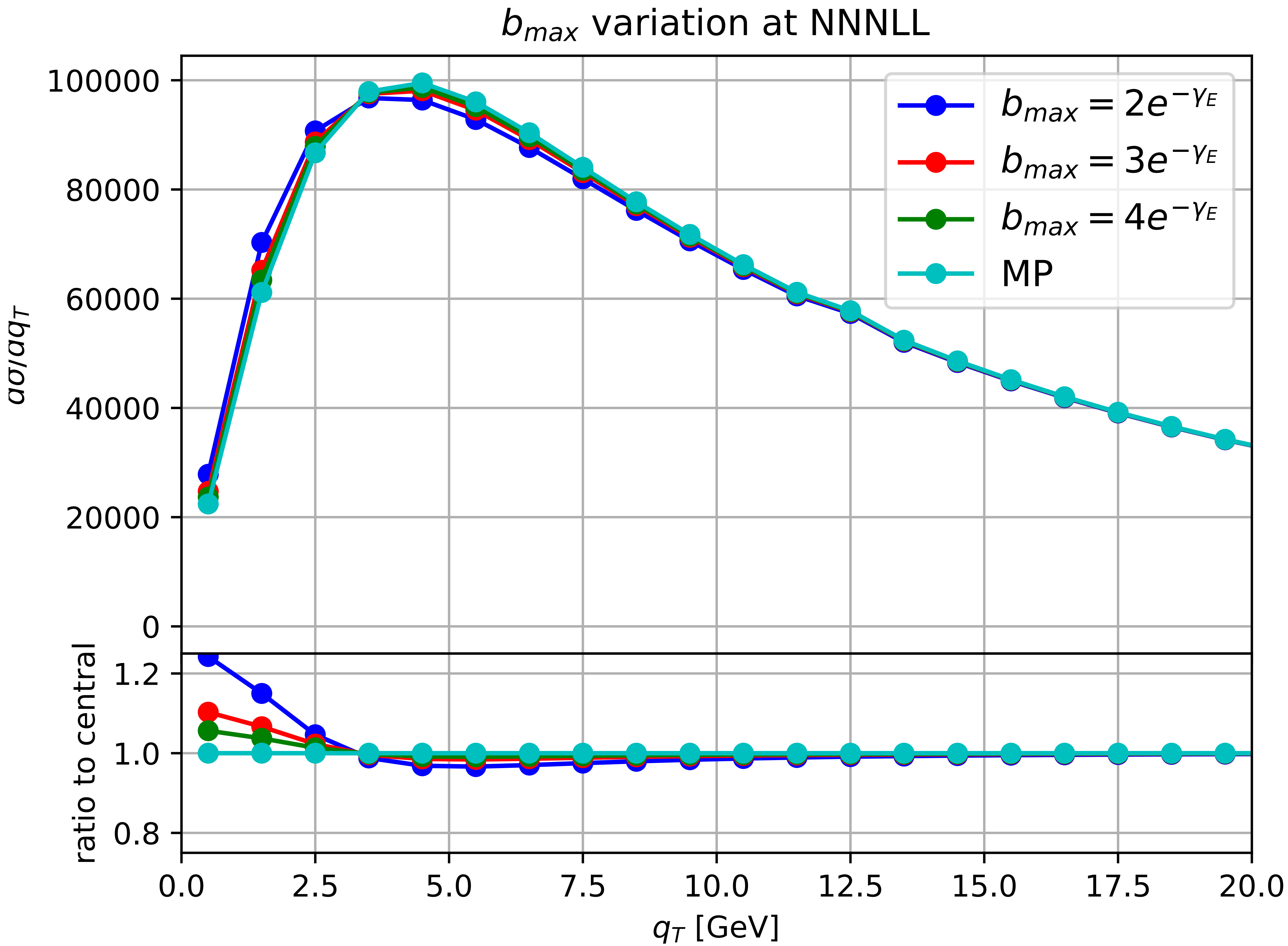

Including $\mathcal{O}(\Lambda_{\rm QCD}/q_T)$ corrections

- **TMD factorisation** is particularly suited to parametrise $\mathcal{O}(\Lambda_{\rm QCD}/q_T)$ (non-perturbative) corrections:

Non-perturbative | Purely perturbative

$$F_i(x, b_T; \mu, \zeta) = \left[\frac{F_i(x, b_T; \mu, \zeta)}{F_i(x, b_*(b_T); \mu, \zeta)}\right] F_i(x, b_*(b_T); \mu, \zeta) \equiv f_{\rm NP}^{(i)}(x, b_T; \zeta) F_i(x, b_*(b_T); \mu, \zeta)$$

- Properties of $f_{\rm NP}$:
  - it has to go to **one** as $b_{\rm T}$ goes to zero: reproduce the perturbative regime,
  - it has to got to **zero** as $b_{\rm T}$ becomes large: mimic the Sudakov suppression,
  - it does *not* depend on μ (ren. scale) but only on ζ (rapidity scale),
  - it is generally **flavour dependent**,
  - the ζ scaling is predictable, and flavour and x independent (Collins-Soper kernel).
- **Important**: $f_{\rm NP}$ is *not universal* as it depends on the specific b_* or, more in general, on the strategy used to regularise the Landau pole.

Including $\mathcal{O}(\Lambda_{\rm QCD}/q_T)$ corrections

- Without loss of generality, $f_{\rm NP}$ can be parametrised as:

$$\boldsymbol{f_{\rm NP}^{(i)}(x, b_T; \zeta) = \exp\left[-g_i(x, b_T) - g_K(b_T)\ln\left(\frac{\zeta}{Q_0^2}\right)\right]}$$

- Given the properties above, there is not a huge latitude in defining $f_{\rm NP}$:
  - both g_i and g_K have to go to zero as b_T tends to zero, and become large as b_T becomes large:
    - $f_{\rm NP}$ can be sensibly different from one only for $b_T^{-1} \lesssim \Lambda_{\rm QCD}^{-1}$ ($k_T \lesssim \Lambda_{\rm QCD}$).
  - g_K (non-perturbative contribution to the Collins-Soper kernel) can be determined faithfully having a **large lever arm** in $\zeta \propto Q$:
    - both **low *and* high invariant-mass data** necessary.
    - **Lattice** simulations available.

Collis-Soper kernel

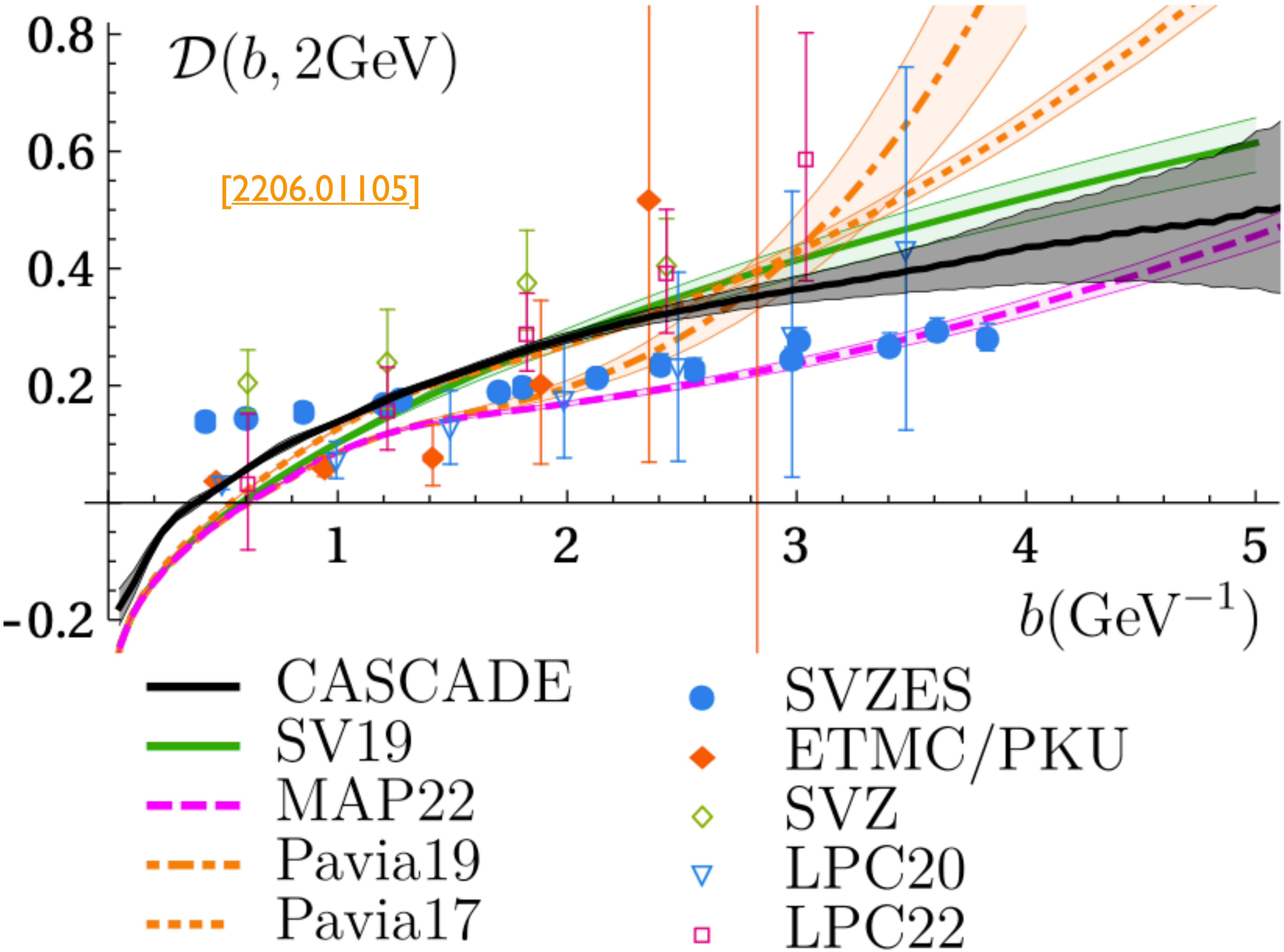

Importance of the *x*-dependence

- However $f_{\rm NP}$ cannot be too simple either!

- In [*JHEP* 07 (2020) 117] a fit of an ***x*-dependent** $f_{\rm NP}$ to a set 353 DY data points was done, obtaining a χ^2 per data point ($\chi^2/N_{\rm dat}$) equal to **1.02**:

- A **gaussian**, ***x*-independent** $f_{\rm NP}$ was also tested:

$$f_{\rm NP}^{\rm DWS}(b_T,\zeta) = \exp\left[-\frac{1}{2}\left(g_1 + g_2\ln\left(\frac{\zeta}{2Q_0^2}\right)\right)b_T^2\right]$$

- This $f_{\rm NP}$ was used to fit the full data set as well as a subset in which rapidity-dependent data (from ATLAS) was excluded:

	Full dataset	No y-differential data
Global $\chi^2/N_{\rm dat}$	1.339	0.895

- **Gaussian ansatz is insufficient** to describe data accurately. Deterioration largely due to the rapidity-dependent data.

Relevance of f_{NP} at high-energies

- In order to assess the relevance of f_{NP} for the description of data at high-energy colliders (Tevatron and LHC), compute the χ^2 of predictions:

  1) setting $f_{\mathrm{NP}} = 1$,

  2) using a fit for f_{NP} (*e.g.* MAP22 [*JHEP* 10 (2022) 127]).

- The theoretical accuracy is $\mathrm{N}^3\mathrm{LL}$.

- The χ^2 accounts for all systematic uncertainties (correlated and uncorrelated) and for collinear PDF uncertainties (MSHT2020).

- A cut $q_T/Q < [q_T/Q]_{\max} = 0.15$ is enforced to ensure to be in the resummation region,

- A cut $q_T/Q > [q_T/Q]_{\min} \in [0,0.1]$ is also enforced to verify that f_{NP} plays a more prominent role for $q_T \lesssim \Lambda_{QCD} \sim 1 - 2$ GeV.

Relevance of $f_{\rm NP}$ at high-energies

Experiment	Observable	$\sqrt{s}$ [GeV]	Q [GeV]	y	Lepton cuts
CDF Run I	$d\sigma/d\|\boldsymbol{q}_T\|$	1800	66 - 116	Inclusive	-
CDF Run II	$d\sigma/d\|\boldsymbol{q}_T\|$	1960	66 - 116	Inclusive	-
D0 Run I	$d\sigma/d\|\boldsymbol{q}_T\|$	1800	75 - 105	Inclusive	-
D0 Run II	$(1/\sigma)d\sigma/d\|\boldsymbol{q}_T\|$	1960	70 - 110	Inclusive	-
D0 Run II (μ)	$(1/\sigma)d\sigma/d\|\boldsymbol{q}_T\|$	1960	65 - 115	$\|y\| < 1.7$	$p_{T\ell} > 15$ GeV $\|\eta_\ell\| < 1.7$
LHCb 7 TeV	$d\sigma/d\|\boldsymbol{q}_T\|$	7000	60 - 120	$2 < y < 4.5$	$p_{T\ell} > 20$ GeV $2 < \eta_\ell < 4.5$
LHCb 8 TeV	$d\sigma/d\|\boldsymbol{q}_T\|$	8000	60 - 120	$2 < y < 4.5$	$p_{T\ell} > 20$ GeV $2 < \eta_\ell < 4.5$
LHCb 13 TeV	$d\sigma/d\|\boldsymbol{q}_T\|$	13000	60 - 120	$2 < y < 4.5$	$p_{T\ell} > 20$ GeV $2 < \eta_\ell < 4.5$
CMS 7 TeV	$(1/\sigma)d\sigma/d\|\boldsymbol{q}_T\|$	7000	60 - 120	$\|y\| < 2.1$	$p_{T\ell} > 20$ GeV $\|\eta_\ell\| < 2.1$
CMS 8 TeV	$(1/\sigma)d\sigma/d\|\boldsymbol{q}_T\|$	8000	60 - 120	$\|y\| < 2.1$	$p_{T\ell} > 15$ GeV $\|\eta_\ell\| < 2.1$
CMS 13 TeV	$d\sigma/d\|\boldsymbol{q}_T\|$	13000	76 - 106	$\|y\| < 0.4$ $0.4 < \|y\| < 0.8$ $0.8 < \|y\| < 1.2$ $1.2 < \|y\| < 1.6$ $1.6 < \|y\| < 2.4$	$p_{T\ell} > 25$ GeV $\|\eta_\ell\| < 2.4$
ATLAS 7 TeV	$(1/\sigma)d\sigma/d\|\boldsymbol{q}_T\|$	7000	66 - 116	$\|y\| < 1$ $1 < \|y\| < 2$ $2 < \|y\| < 2.4$	$p_{T\ell} > 20$ GeV $\|\eta_\ell\| < 2.4$
ATLAS 8 TeV on-peak	$(1/\sigma)d\sigma/d\|\boldsymbol{q}_T\|$	8000	66 - 116	$\|y\| < 0.4$ $0.4 < \|y\| < 0.8$ $0.8 < \|y\| < 1.2$ $1.2 < \|y\| < 1.6$ $1.6 < \|y\| < 2$ $2 < \|y\| < 2.4$	$p_{T\ell} > 20$ GeV $\|\eta_\ell\| < 2.4$
ATLAS 8 TeV off-peak	$(1/\sigma)d\sigma/d\|\boldsymbol{q}_T\|$	8000	46 - 66 116 - 150	$\|y\| < 2.4$	$p_{T\ell} > 20$ GeV $\|\eta_\ell\| < 2.4$
ATLAS 13 TeV	$(1/\sigma)d\sigma/d\|\boldsymbol{q}_T\|$	13000	66 - 113	$\|y\| < 2.5$	$p_{T\ell} > 27$ GeV $\|\eta_\ell\| < 2.5$

Relevance of $f_{\rm NP}$ at high-energies

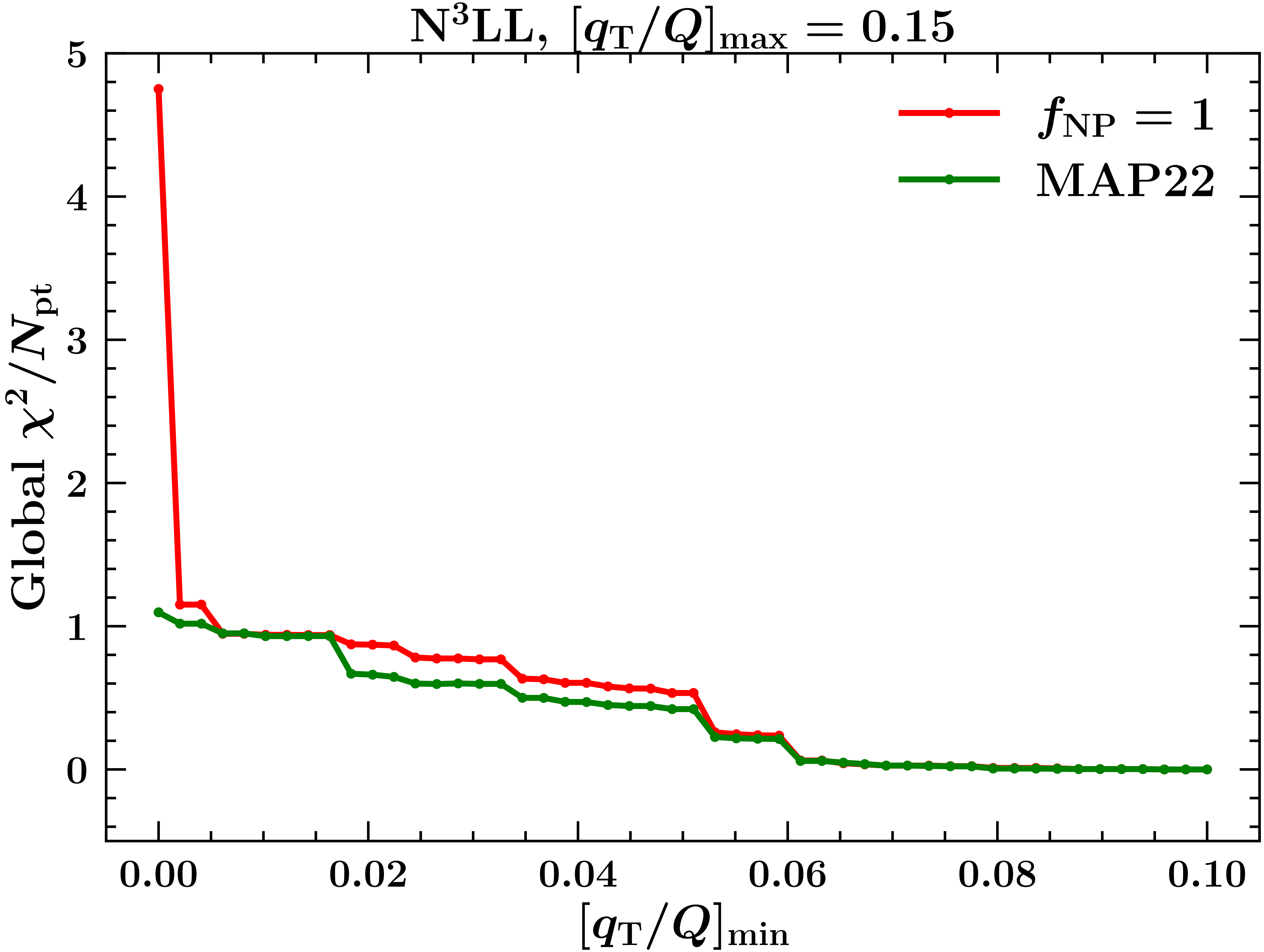

Relevance of f_{NP} at high-energies

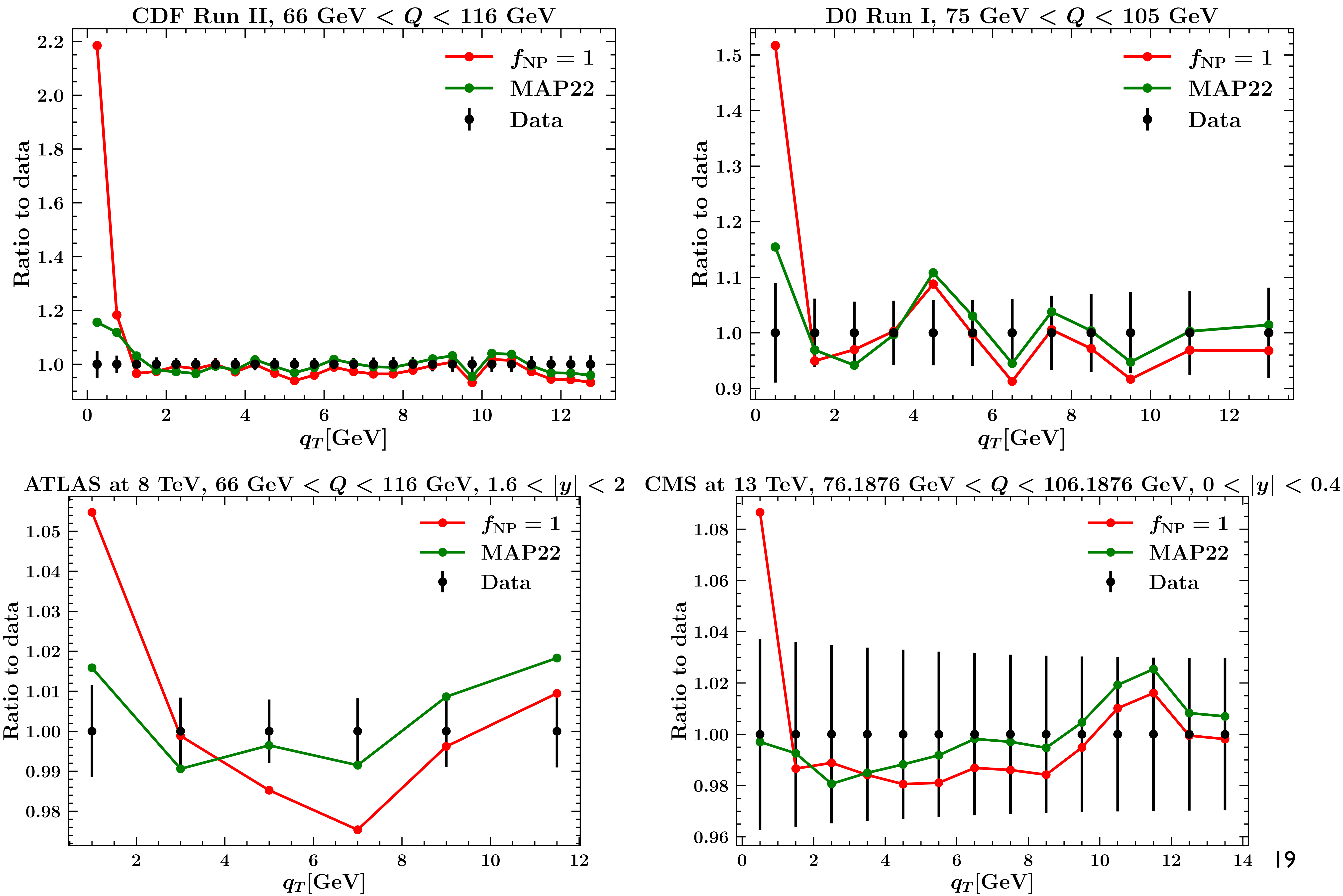

Conclusions

- **Non perturbative effects** that scale like a power of $\Lambda_{\rm QCD}/q_T$ are sizeable at small q_T, that is the domain of resummation,
    - necessary to describe the first bins in q_T of high-energy data,
- **TMD factorisation** is just one of the possible ways to resum large logs of q_T, but it is particularly suited to study non-perturbative effects.
- within TMD factorisation, different **extractions from data** of these effects as encoded in $f_{\rm NP}$ have been performed.
- In doing so, several aspects have to be considered:
    - regularisation, parameterisation of $f_{\rm NP}$, flavour dependence, etc.
- All of them have to be accounted for to achieve reliable predictions.

Backup

Origin of $\mathcal{O}(\Lambda_{\rm QCD}/q_T)$ corrections

- Within the context of the b_* prescription, **different recipes** exist:
  - Replace $b_T \to b_*(b_T)$ everywhere in the calculation (including where it is not strictly needed to regulate the Landau pole) $\Rightarrow$ **Global b_* prescription**
  - Replace $b_T \to b_*(b_T)$ only where strictly need to regulate the Landau pole (*i.e.* in the running of α_s and PDFs) $\Rightarrow$ **Local b_* prescription**

Origin of $\mathcal{O}(\Lambda_{\mathrm{QCD}}/q_T)$ corrections

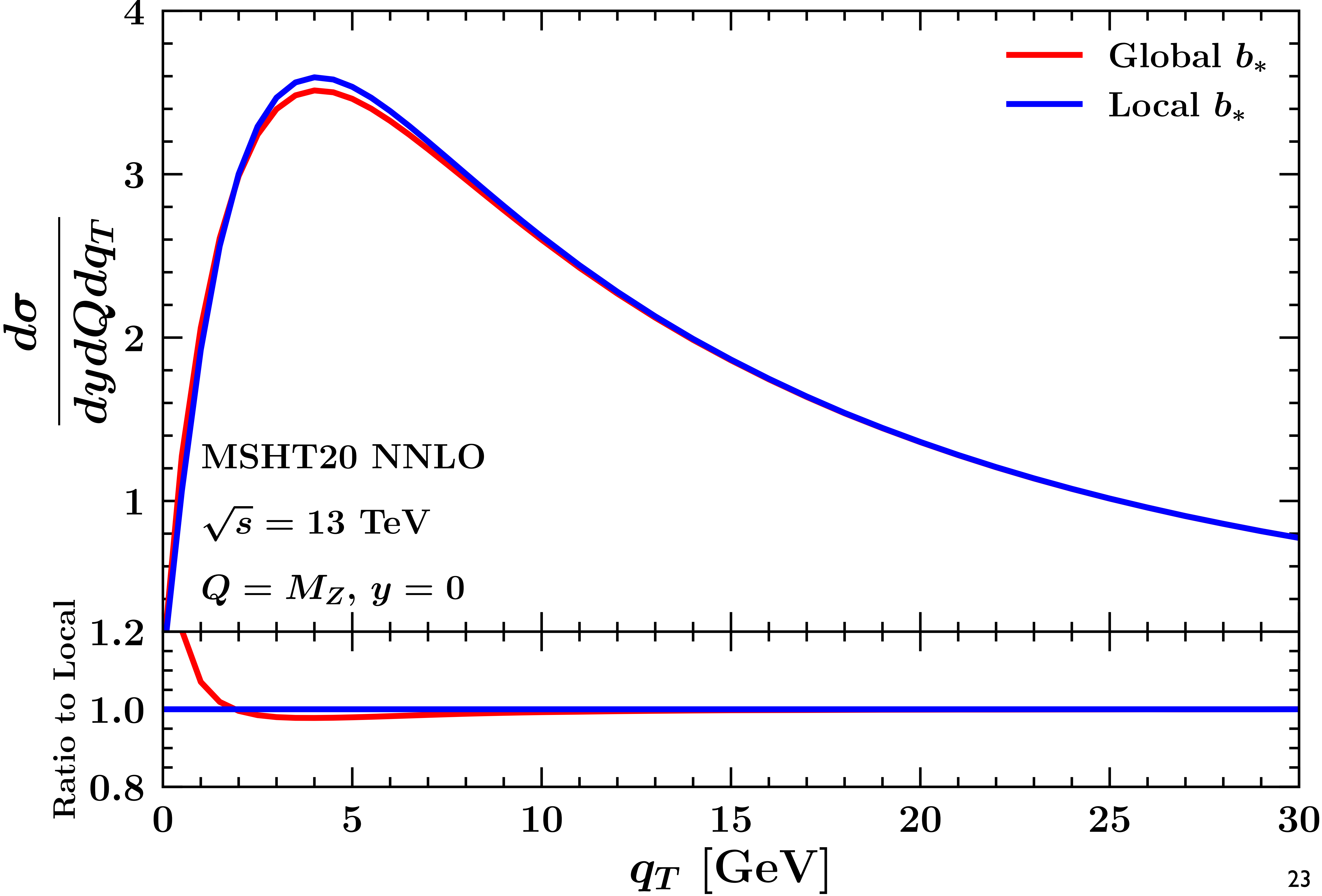

Heavy-quark masses/thresholds

- Usually, the resummation of logs of q_T does not account for the finiteness of **heavy-quark (charm and bottom) masses** m_h:
  - a fully consistent calculation accounting for heavy-quark masses is hard to achieve,
  - however these affects are expected to be relevant when $q_T \lesssim m_h$.
- Indeed, most of the calculations are performed in the **massless** scheme.
- The massless scheme introduces an explicit dependence of the relevant quantities on the number of active flavours n_f:
  - a partial account of heavy-quark mass effects can be achieved by **varying** n_f at the heavy-quark thresholds depending on the scale at which each quantity is computed.
- For example:

$$F^{(4)}(\mu) = e^{S^{(4)}(\mu,m_h)} e^{S^{(3)}(m_h,\mu_b)} [C^{(3)} \otimes f^{(3)}](\mu_b)\,, \quad \mu_b < m_h < \mu$$

- where $\mu_b = b_0/b_T$ with b_T to be integrated over.

Heavy-quark masses/thresholds

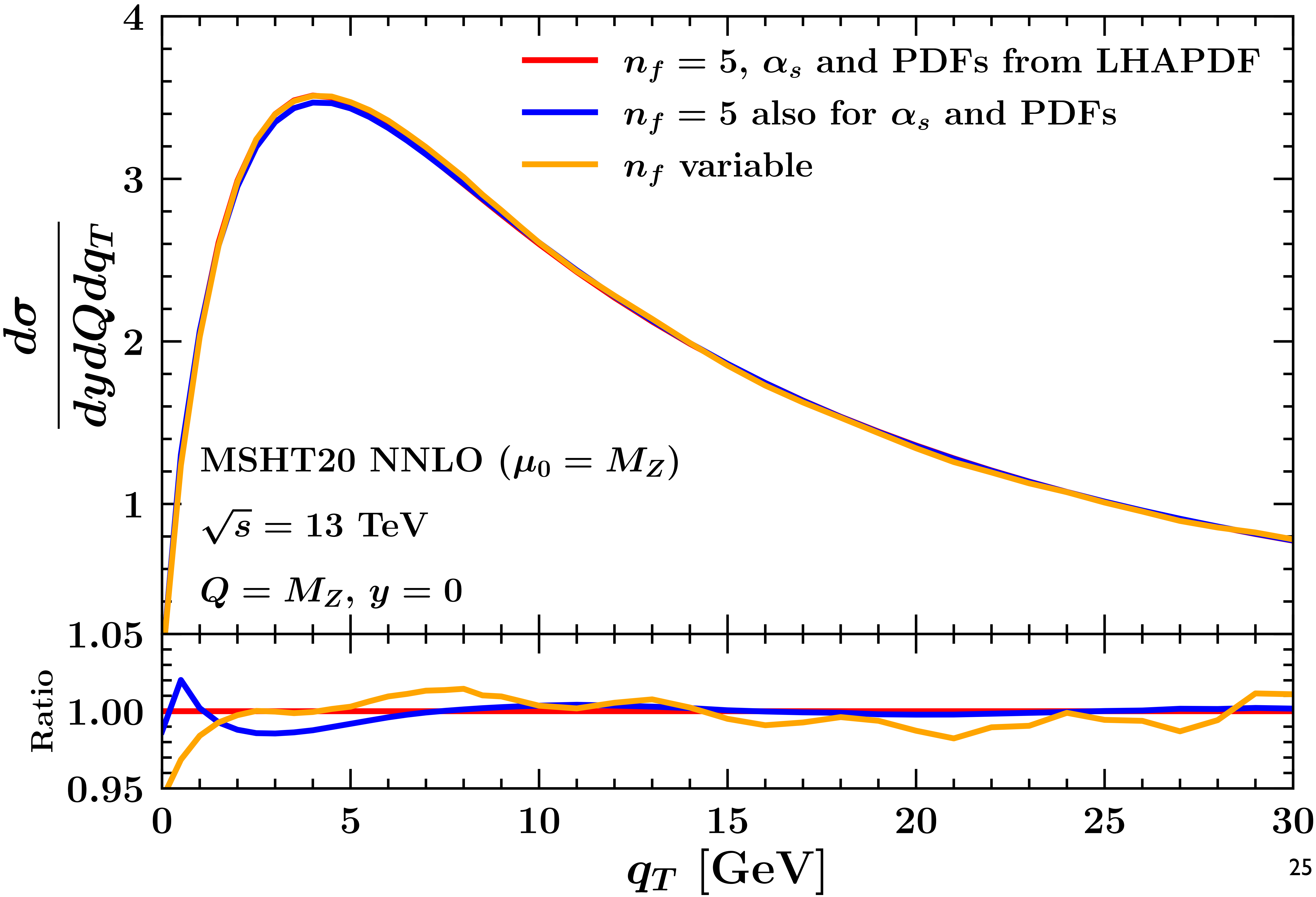

Collis-Soper kernel

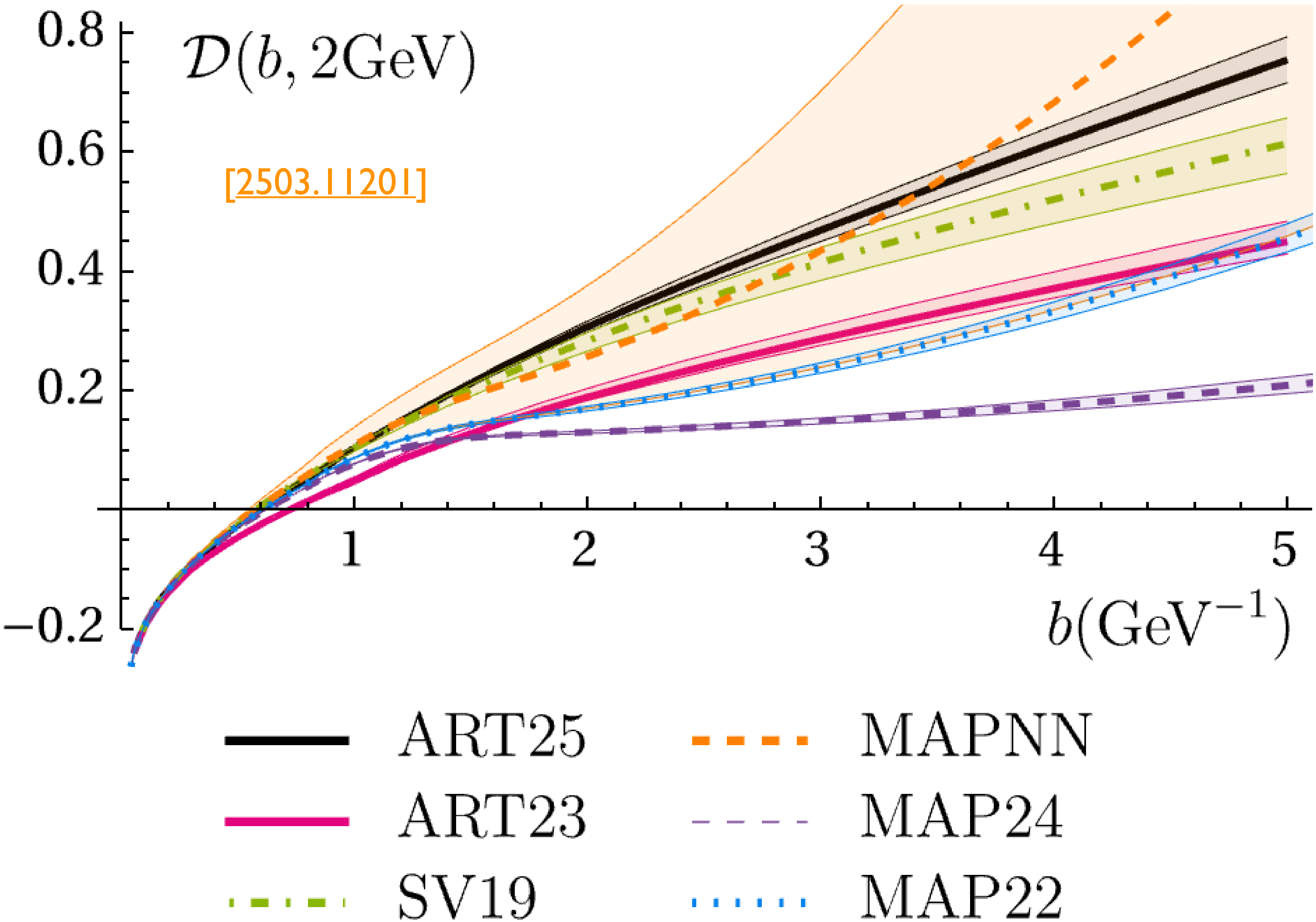

Perturbative convergence

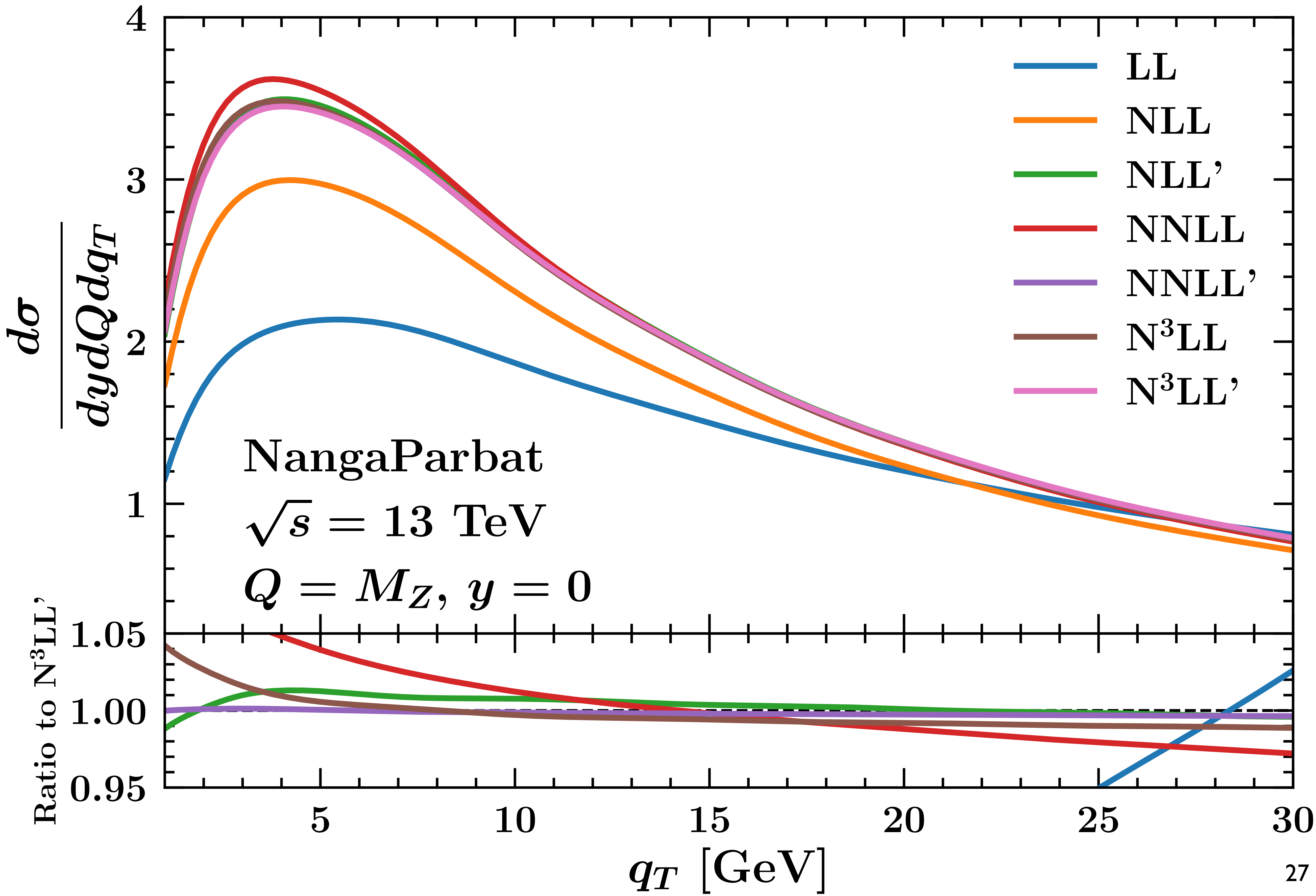

Flavour dependence of $f_{\rm NP}$

- For each TMD use a **Gaussian ansatz**:

$$f_{\rm NP}(b_T, \zeta) = \exp\left[-g_a b_T^2 - g_K b_T^2 \ln\left(\frac{\zeta}{Q_0^2}\right)\right]$$

- **1 flavour-independent set** with $g_a = 0.4\ \mathrm{GeV}^2$, [Guzzi, Nadolsky, Wang (2014)]
- **50 flavour-dependent sets** with $\{g_{u_v}, g_{d_v}, g_{u_s}, g_{d_s}, g_s\}$, $g_a \in [0.2, 0.6]\ \mathrm{GeV}^2$,
- keep g_K fixed. [Bacchetta, Delcarro, Pisano, Radici, Signori (2017)]

Bacchetta, Bozzi, Radici, Ritzmann, Signori
PLB 788, 542 (2019)

“Z-equivalent” sets

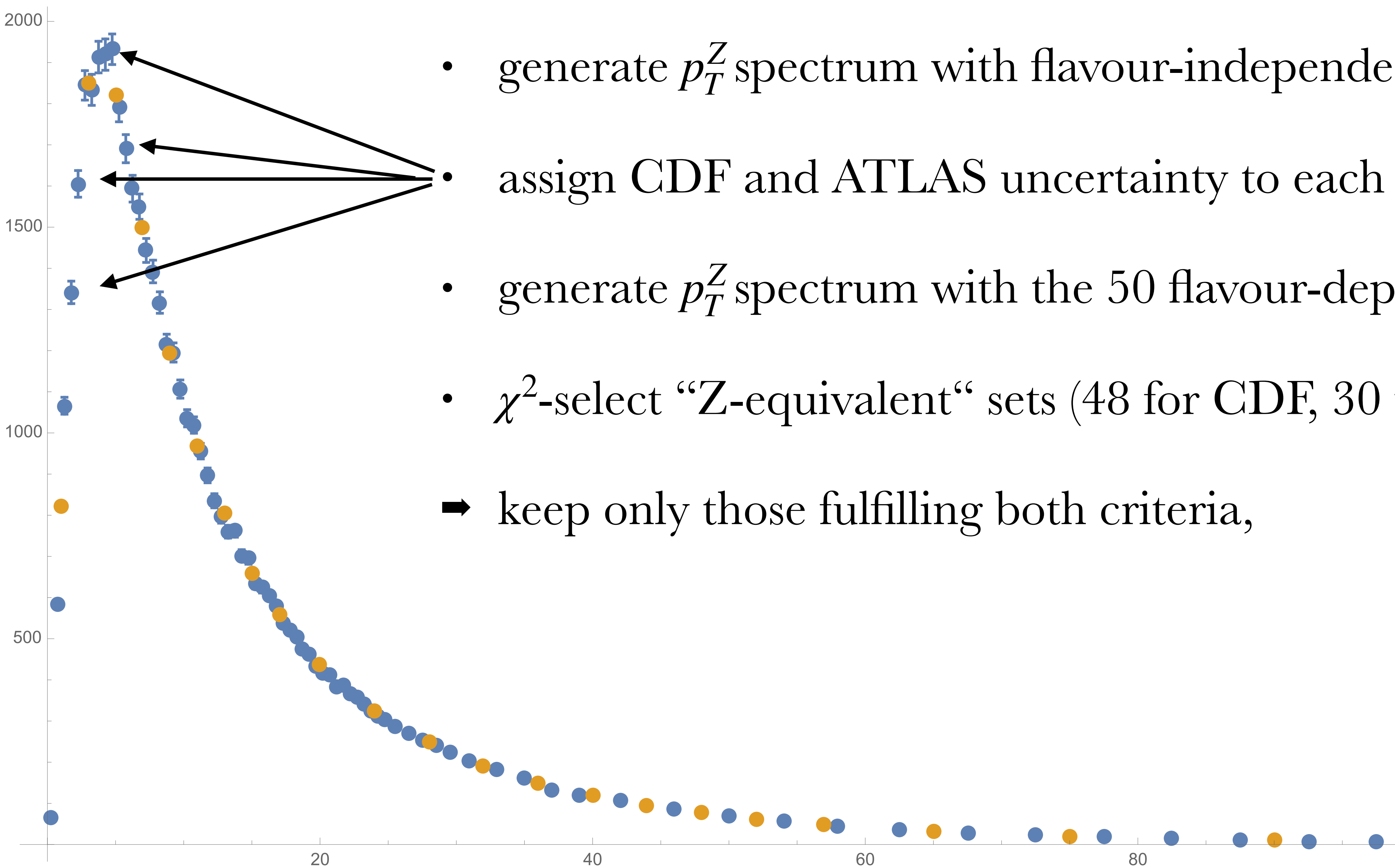

- generate p_T^Z spectrum with flavour-independent set,
- assign CDF and ATLAS uncertainty to each bin,
- generate p_T^Z spectrum with the 50 flavour-dependent sets,
- χ^2-select “Z-equivalent“ sets (48 for CDF, 30 for ATLAS),

➡ keep only those fulfilling both criteria,

Bacchetta, Bozzi, Radici, Ritzmann, Signori
PLB 788, 542 (2019)

Impact on m_W

- Take the "Z-equivalent" *flavour-dependent* parameter sets and compute *low-statistics* (135M) m_T, p_T^l, p_T^ν distributions

  ➡ **pseudodata**

- Take the *flavour-independent* parameter set and compute *high-statistics* (750M) m_T, p_T^l, p_T^ν distributions for 30 different values of M_W

  ➡ **templates**

- **perform the template fit procedure and compute the shifts induced by flavour effects**

- transverse mass: zero or few MeV shifts, generally favouring lower values for W^- (preferred by EW fit)

- lepton pt: quite important shifts (envelope **up to 15 MeV**)

- neutrino pt: same order of magnitude (or bigger) as lepton pt

	ΔM_{W+}			ΔM_{W-}		
Set	m_T	$p_{T\ell}$	$p_{T\nu}$	m_T	$p_{T\ell}$	$p_{T\nu}$
1	0	-1	-2	-2	3	-3
2	0	-6	0	-2	0	-5
3	-1	9	0	-2	4	-10
4	0	0	-2	-2	-4	-10
5	0	4	1	-1	-3	-6
6	1	0	2	-1	4	-4
7	2	-1	2	-1	0	-8
8	0	2	8	1	7	8
9	0	4	-3	-1	0	7

TABLE I: ATLAS 7 TeV

	ΔM_{W+}			ΔM_{W-}		
Set	m_T	$p_{T\ell}$	$p_{T\nu}$	m_T	$p_{T\ell}$	$p_{T\nu}$
1	-1	-5	7	-1	-3	8
2	-1	-15	6	0	5	10
3	-1	1	8	-1	-7	5
4	-1	-15	6	0	-4	5
5	-1	-4	6	-1	-7	5
6	-1	-5	7	0	2	9
7	-1	-15	6	-1	-6	5
8	-1	0	8	0	3	10
9	-1	-7	7	0	4	10

TABLE II: LHCb 13 TeV

Set	u_v	d_v	u_s	d_s	s
1	0.34	0.26	0.46	0.59	0.32
2	0.34	0.46	0.56	0.32	0.51
3	0.55	0.34	0.33	0.55	0.30
4	0.53	0.49	0.37	0.22	0.52
5	0.42	0.38	0.29	0.57	0.27
6	0.40	0.52	0.46	0.54	0.21
7	0.22	0.21	0.40	0.46	0.49
8	0.53	0.31	0.59	0.54	0.33
9	0.46	0.46	0.58	0.40	0.28

Statistical uncertainty: 2.5 MeV

Bacchetta, Bozzi, Radici, Ritzmann, Signori
PLB 788, 542 (2019)

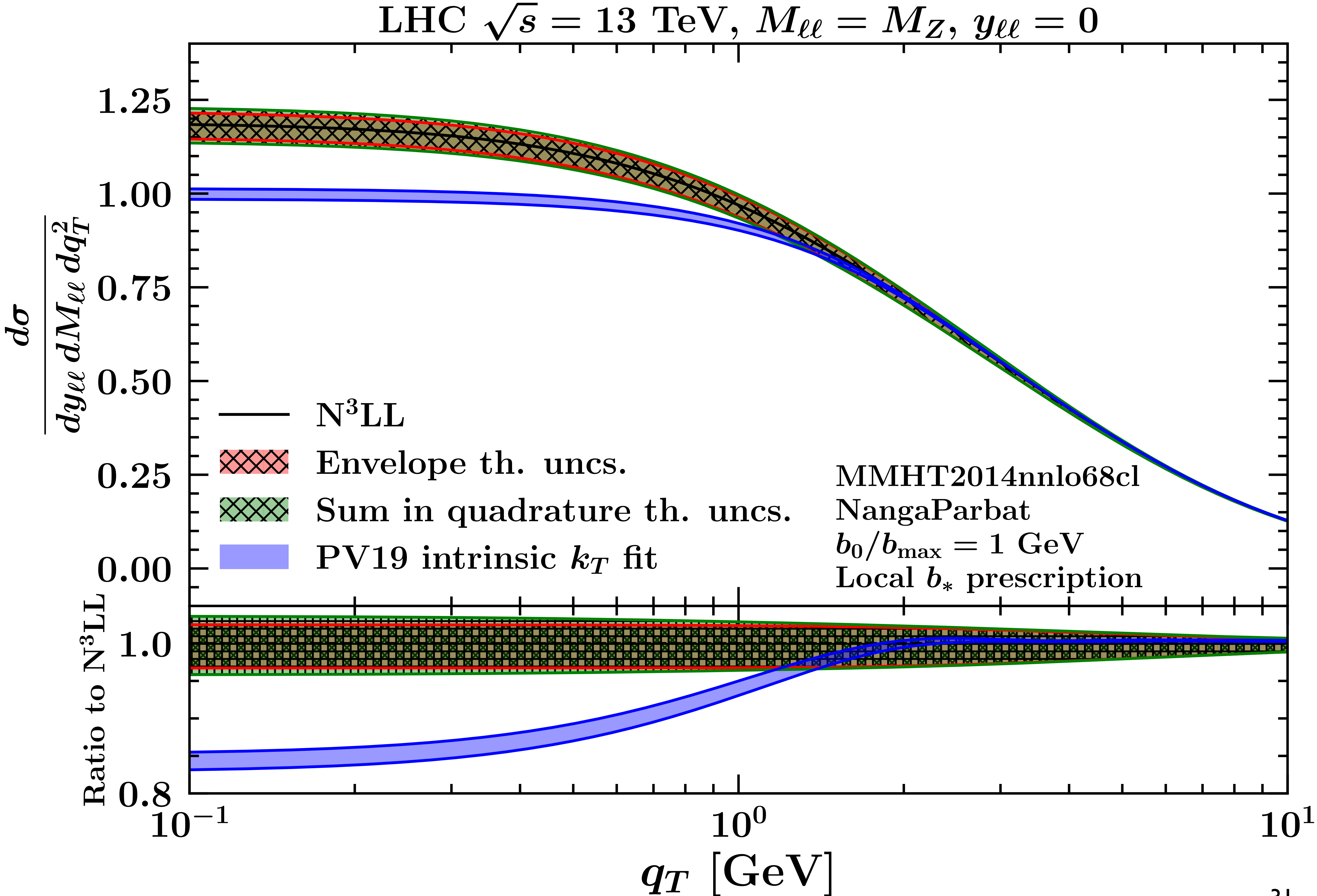

LHC $\sqrt{s} = 13$ TeV, $M_{\ell\ell} = M_Z$, $y_{\ell\ell} = 0$
$\frac{d\sigma}{dy_{\ell\ell}\, dM_{\ell\ell}\, dq_T^2}$
N^{3}LL
Envelope th. uncs.
Sum in quadrature th. uncs.
PV19 intrinsic k_T fit
MMHT2014nnlo68cl
NangaParbat
$b_0/b_{\max} = 1$ GeV
Local b_* prescription
Ratio to N^{3}LL
q_T [GeV]

TMD factorisation

- TMD factorisation introduces two independent scales:
  - the **renormalisation scale μ**, originating from the UV renormalisation,
  - the **rapidity scale ζ**, originating from the cancellation of rapidity divergences.
- The respective **evolution equations** are:

$$\frac{\partial \ln F}{\partial \ln \sqrt{\zeta}} = K(\mu_0) - \int_{\mu_0}^{\mu} \frac{d\mu'}{\mu'} \gamma_K(\alpha_s(\mu'))$$

$$\frac{\partial \ln F}{\partial \ln \mu} = \gamma_F(\alpha_s(\mu)) - \gamma_K(\alpha_s(\mu)) \ln \frac{\sqrt{\zeta}}{\mu}$$

- At small $b_{\rm T}$, TMDs can be matched onto collinear distributions:

$$F(\mu, \zeta) = C(\mu, \zeta) \otimes f(\mu)$$

- The solution final is:

$\mu_b = b_0 / b_{\rm T}$

$$F(\mu,\zeta) = \exp\left\{K(\mu_0)\ln\frac{\sqrt{\zeta}}{\sqrt{\zeta_0}} + \int_{\mu_0}^{\mu}\frac{d\mu'}{\mu'}\left[\gamma_F(\alpha_s(\mu')) - \gamma_K(\alpha_s(\mu'))\ln\frac{\sqrt{\zeta}}{\mu'}\right]\right\} C(\mu_0,\zeta_0)\otimes f(\mu_0)$$

- Anomalous dims. and matching funcs. **perturbatively** computable.

TMD factorisation

- Final expression:

$$
\begin{aligned}
F_{f/P}(x, \mathbf{b}_T; \mu, \zeta) &= \sum_j C_{f/j}(x, b_*; \mu_b, \mu_b^2) \otimes f_{j/P}(x, \mu_b) && : A \\
&\times \exp\left\{ K(b_*; \mu_b) \ln \frac{\sqrt{\zeta}}{\mu_b} + \int_{\mu_b}^{\mu} \frac{d\mu'}{\mu'} \left[\gamma_F - \gamma_K \ln \frac{\sqrt{\zeta}}{\mu'} \right] \right\} && : B \\
&\times \exp\left\{ g_{j/P}(x, b_T) + g_K(b_T) \ln \frac{\sqrt{\zeta_F}}{\sqrt{\zeta_{F,0}}} \right\} && : C
\end{aligned}
$$

- matching onto the collinear region at $b_T \ll 1/\Lambda_{QCD}$,
- factorises as *hard* (perturbative) and *longitudinal* (*i.e.* collinear, non-perturbative).

- CS and RGE evolution,
- evolution in μ and ζ,
- perturbative.

- avoid the Landau pole,
- f_{NP} accounts for the introduction of b_*,
- f_{NP} is non-perturbative thus **fit** to data.

Logarithmic counting

$$\left(\frac{d\sigma}{dq_T}\right)_{\text{res.}} \overset{\text{TMD}}{=} \sigma_0 H(Q) \int d^2\mathbf{b}_T e^{i\mathbf{b}_T\cdot\mathbf{q}_T} F_1(x_1,\mathbf{b}_T,Q,Q^2) F_2(x_2,\mathbf{b}_T,Q,Q^2)$$

$$F_i = \sum_j \left(C_{i/j}\otimes f_j\right) \exp\left\{K \ln\frac{\sqrt{\zeta}}{\mu_b} + \int_{\mu_b}^{\mu} \frac{d\mu'}{\mu'}\left[\gamma_F - \gamma_K \ln\frac{\sqrt{\zeta}}{\mu'}\right]\right\}$$

Accuracy	γ_K	γ_F	K	$C_{f/j}$	H	FFs/PDFs/α_s
LL	α_s	-	-	1	1	-
NLL	α_s^2	α_s	α_s	1	1	LO
NLL'	α_s^2	α_s	α_s	α_s	α_s	LO
N^2LL	α_s^3	α_s^2	α_s^2	α_s	α_s	NLO
N^2LL'	α_s^3	α_s^2	α_s^2	α_s^2	α_s^2	NLO
N^3LL	α_s^4	α_s^3	α_s^3	α_s^2	α_s^2	NNLO
N^3LL'	α_s^4	α_s^3	α_s^3	α_s^3	α_s^3	NNLO

TMD, q_T resummation, SCET

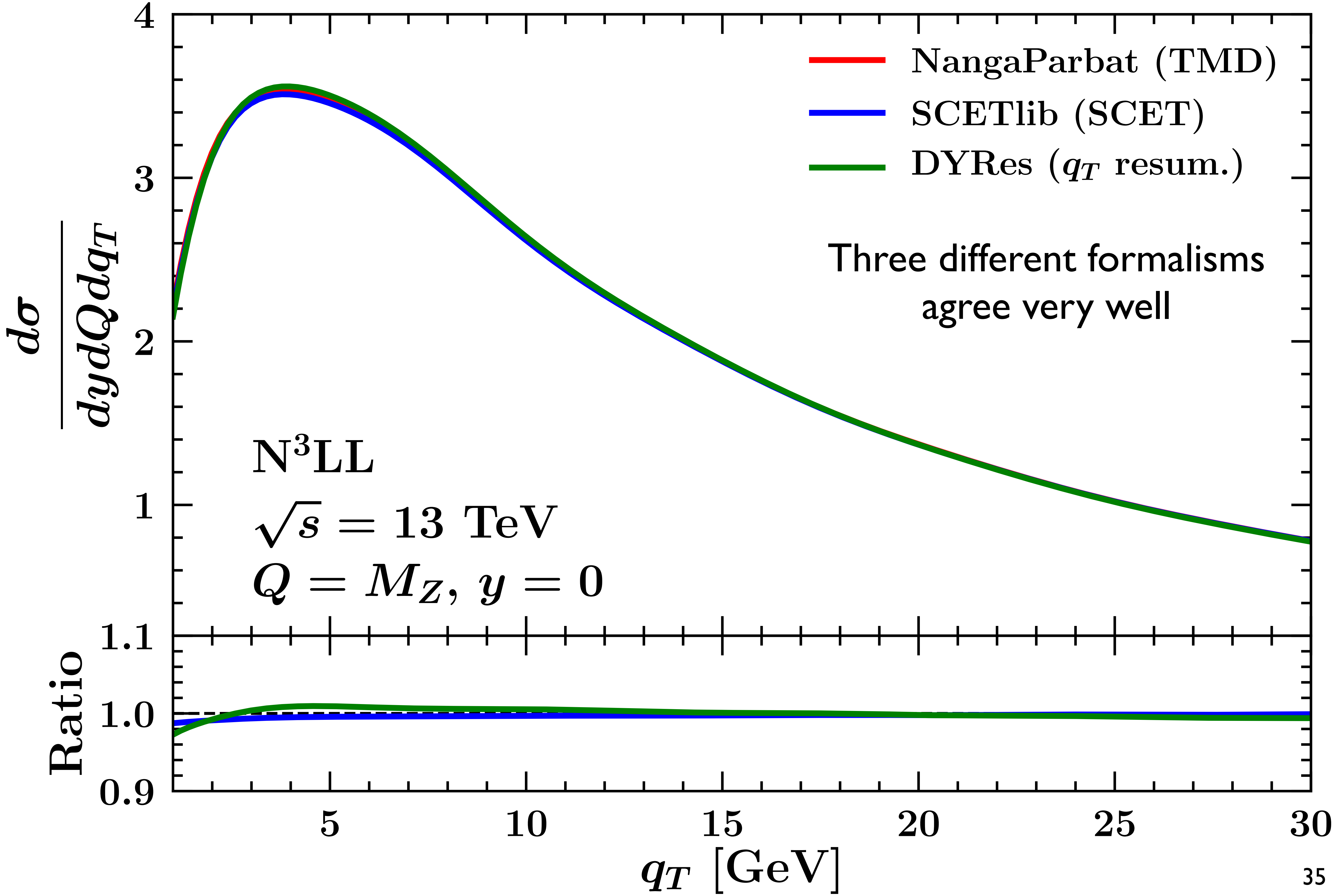

MAPTMD 2022

Main settings

- b_* prescription:

$$b_*(b_T) = b_{\max}\left(\frac{1-e^{-b_T^4/b_{\max}^4}}{1-e^{-b_T^4/b_{\min}^4}}\right)^{1/4} \quad \text{with} \quad \begin{cases} b_{\max} = 2e^{-\gamma_E} \\ b_{\min} = b_{\max}/Q \end{cases}$$

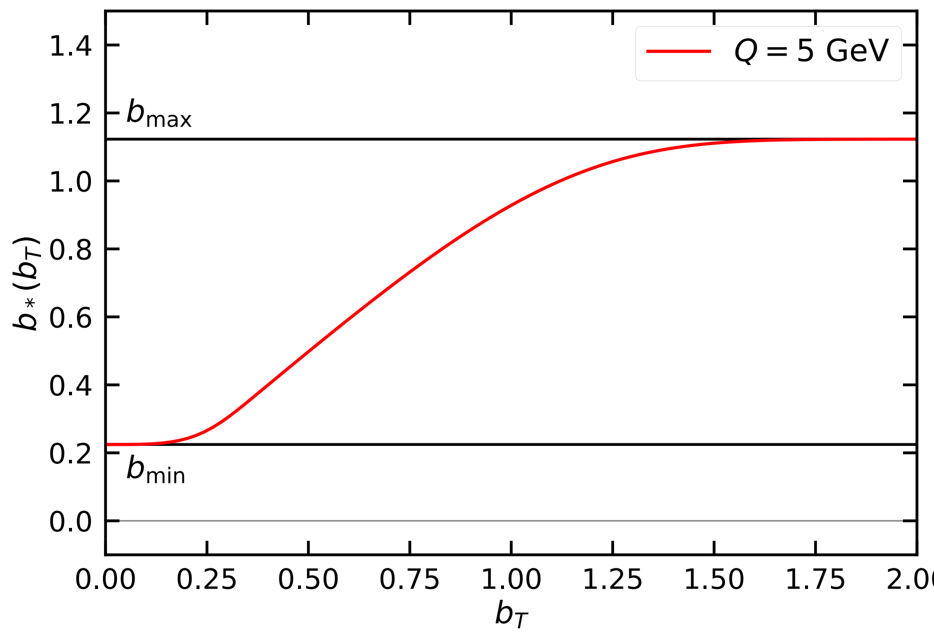

- Non-perturbative function f_{NP}:
  - evolution (CS kernel): $g_K(\boldsymbol{b}_T^2) = -g_2^2\,\frac{\boldsymbol{b}_T^2}{2}$
  - PDFs:

$$f_{1\,NP}(x,\boldsymbol{b}_T^2;\zeta,Q_0) = \frac{g_1(x)\,e^{-g_1(x)\frac{\boldsymbol{b}_T^2}{4}} + \lambda^2\,g_{1B}^2(x)\left[1-g_{1B}(x)\frac{\boldsymbol{b}_T^2}{4}\right]e^{-g_{1B}(x)\frac{\boldsymbol{b}_T^2}{4}} + \lambda_2^2\,g_{1C}(x)\,e^{-g_{1C}(x)\frac{\boldsymbol{b}_T^2}{4}}}{g_1(x)+\lambda^2\,g_{1B}^2(x)+\lambda_2^2\,g_{1C}(x)}\left[\frac{\zeta}{Q_0^2}\right]^{g_K(\boldsymbol{b}_T^2)/2}$$

  - FFs:

$$D_{1\,NP}(z,\boldsymbol{b}_T^2;\zeta,Q_0) = \frac{g_3(z)\,e^{-g_3(z)\frac{\boldsymbol{b}_T^2}{4z^2}} + \frac{\lambda_F}{z^2}\,g_{3B}^2(z)\left[1-g_{3B}(z)\frac{\boldsymbol{b}_T^2}{4z^2}\right]e^{-g_{3B}(z)\frac{\boldsymbol{b}_T^2}{4z^2}}}{g_3(z)+\frac{\lambda_F}{z^2}\,g_{3B}^2(z)}\left[\frac{\zeta}{Q_0^2}\right]^{g_K(\boldsymbol{b}_T^2)/2}$$

$$g_{\{1,1B,1C\}}(x) = N_{\{1,1B,1C\}}\frac{x^{\sigma_{\{1,2,3\}}}(1-x)^{\alpha^2_{\{1,2,3\}}}}{\hat{x}^{\sigma_{\{1,2,3\}}}(1-\hat{x})^{\alpha^2_{\{1,2,3\}}}} \qquad g_{\{3,3B\}}(z) = N_{\{3,3B\}}\frac{(z^{\beta_{\{1,2\}}}+\delta^2_{\{1,2\}})(1-z)^{\gamma^2_{\{1,2\}}}}{(\hat{z}^{\beta_{\{1,2\}}}+\delta^2_{\{1,2\}})(1-\hat{z})^{\gamma^2_{\{1,2\}}}}$$

- 11 (PDFs) + 9 (FFs) + 1 (evol): **21 free parameters** to fit to data.
- Perturbative accuracies: **N^{3}LL(-)**.
- **Monte Carlo** method for the experimental error propagation.

MAPTMD 2022

Dataset

- DY data:
  - fixed-target low-energy DY,
  - RHIC data,
  - LHC and Tevatron data,
  - selection cut $q_T / Q < 0.2$,
  - 484 data points.
- SIDIS data:
  - HERMES and COMPASS,
  - $P_{hT}|_{\max} = \min[\min[0.2Q, 0.5zQ] + 0.3 \text{ GeV}, zQ]$
  - $Q > 1.4$ GeV, $0.2 < z < 0.7$,
  - 1547 points.

Experiment	$N_{\rm dat}$	Observable	$\sqrt{s}$ [GeV]	Q [GeV]	y or x_F	Lepton cuts	Ref.
E605	50	$Ed^3\sigma/d^3\boldsymbol{q}$	38.8	7 - 18	$x_F = 0.1$	-	[55]
E772	53	$Ed^3\sigma/d^3\boldsymbol{q}$	38.8	5 - 15	$0.1 < x_F < 0.3$	-	[51]
E288 200 GeV	30	$Ed^3\sigma/d^3\boldsymbol{q}$	19.4	4 - 9	$y = 0.40$	-	[56]
E288 300 GeV	39	$Ed^3\sigma/d^3\boldsymbol{q}$	23.8	4 - 12	$y = 0.21$	-	[56]
E288 400 GeV	61	$Ed^3\sigma/d^3\boldsymbol{q}$	27.4	5 - 14	$y = 0.03$	-	[56]
STAR 510	7	$d\sigma/d\|\boldsymbol{q}_T\|$	510	73 - 114	$\|y\| < 1$	$p_{T\ell} > 25$ GeV $\|\eta_\ell\| < 1$	-
PHENIX200	2	$d\sigma/d\|\boldsymbol{q}_T\|$	200	4.8 - 8.2	$1.2 < y < 2.2$	-	[52]
CDF Run I	25	$d\sigma/d\|\boldsymbol{q}_T\|$	1800	66 - 116	Inclusive	-	[57]
CDF Run II	26	$d\sigma/d\|\boldsymbol{q}_T\|$	1960	66 - 116	Inclusive	-	[58]
D0 Run I	12	$d\sigma/d\|\boldsymbol{q}_T\|$	1800	75 - 105	Inclusive	-	[59]
D0 Run II	5	$(1/\sigma)d\sigma/d\|\boldsymbol{q}_T\|$	1960	70 - 110	Inclusive	-	[60]
D0 Run II (μ)	3	$(1/\sigma)d\sigma/d\|\boldsymbol{q}_T\|$	1960	65 - 115	$\|y\| < 1.7$	$p_{T\ell} > 15$ GeV $\|\eta_\ell\| < 1.7$	[61]
LHCb 7 TeV	7	$d\sigma/d\|\boldsymbol{q}_T\|$	7000	60 - 120	$2 < y < 4.5$	$p_{T\ell} > 20$ GeV $2 < \eta_\ell < 4.5$	[62]
LHCb 8 TeV	7	$d\sigma/d\|\boldsymbol{q}_T\|$	8000	60 - 120	$2 < y < 4.5$	$p_{T\ell} > 20$ GeV $2 < \eta_\ell < 4.5$	[63]
LHCb 13 TeV	7	$d\sigma/d\|\boldsymbol{q}_T\|$	13000	60 - 120	$2 < y < 4.5$	$p_{T\ell} > 20$ GeV $2 < \eta_\ell < 4.5$	[64]
CMS 7 TeV	4	$(1/\sigma)d\sigma/d\|\boldsymbol{q}_T\|$	7000	60 - 120	$\|y\| < 2.1$	$p_{T\ell} > 20$ GeV $\|\eta_\ell\| < 2.1$	[65]
CMS 8 TeV	4	$(1/\sigma)d\sigma/d\|\boldsymbol{q}_T\|$	8000	60 - 120	$\|y\| < 2.1$	$p_{T\ell} > 15$ GeV $\|\eta_\ell\| < 2.1$	[66]
CMS 13 TeV	70	$d\sigma/d\|\boldsymbol{q}_T\|$	13000	76 - 106	$\|y\| < 0.4$ $0.4 < \|y\| < 0.8$ $0.8 < \|y\| < 1.2$ $1.2 < \|y\| < 1.6$ $1.6 < \|y\| < 2.4$	$p_{T\ell} > 25$ GeV $\|\eta_\ell\| < 2.4$	[53]
ATLAS 7 TeV	6 6 6	$(1/\sigma)d\sigma/d\|\boldsymbol{q}_T\|$	7000	66 - 116	$\|y\| < 1$ $1 < \|y\| < 2$ $2 < \|y\| < 2.4$	$p_{T\ell} > 20$ GeV $\|\eta_\ell\| < 2.4$	[67]
ATLAS 8 TeV on-peak	6 6 6 6 6 6	$(1/\sigma)d\sigma/d\|\boldsymbol{q}_T\|$	8000	66 - 116	$\|y\| < 0.4$ $0.4 < \|y\| < 0.8$ $0.8 < \|y\| < 1.2$ $1.2 < \|y\| < 1.6$ $1.6 < \|y\| < 2$ $2 < \|y\| < 2.4$	$p_{T\ell} > 20$ GeV $\|\eta_\ell\| < 2.4$	[68]
ATLAS 8 TeV off-peak	4 8	$(1/\sigma)d\sigma/d\|\boldsymbol{q}_T\|$	8000	46 - 66 116 - 150	$\|y\| < 2.4$	$p_{T\ell} > 20$ GeV $\|\eta_\ell\| < 2.4$	[68]
ATLAS 13 TeV	6	$(1/\sigma)d\sigma/d\|\boldsymbol{q}_T\|$	13000	66 - 113	$\|y\| < 2.5$	$p_{T\ell} > 27$ GeV $\|\eta_\ell\| < 2.5$	[54]
Total	484						

Experiment	$N_{\rm dat}$	Observable	Channels	Q [GeV]	x	z	Phase space cuts	Ref.
HERMES	344	$M(x, z, \|\boldsymbol{P}_{hT}\|, Q)$	$p \to \pi^+$ $p \to \pi^-$ $p \to K^+$ $p \to K^-$ $d \to \pi^+$ $d \to \pi^-$ $d \to K^+$ $d \to K^-$	1 - $\sqrt{15}$	$0.023 < x < 0.6$ (6 bins)	$0.1 < z < 1.1$ (8 bins)	$W^2 > 10$ GeV^2 $0.1 < y < 0.85$	[46]
COMPASS	1203	$M(x, z, \boldsymbol{P}_{hT}^2, Q)$	$d \to h^+$ $d \to h^-$	1 - 9 (5 bins)	$0.003 < x < 0.4$ (8 bins)	$0.2 < z < 0.8$ (4 bins)	$W^2 > 25$ GeV^2 $0.1 < y < 0.9$	[72]
Total	1547							

MAPTMD 2022

Kinematic coverage

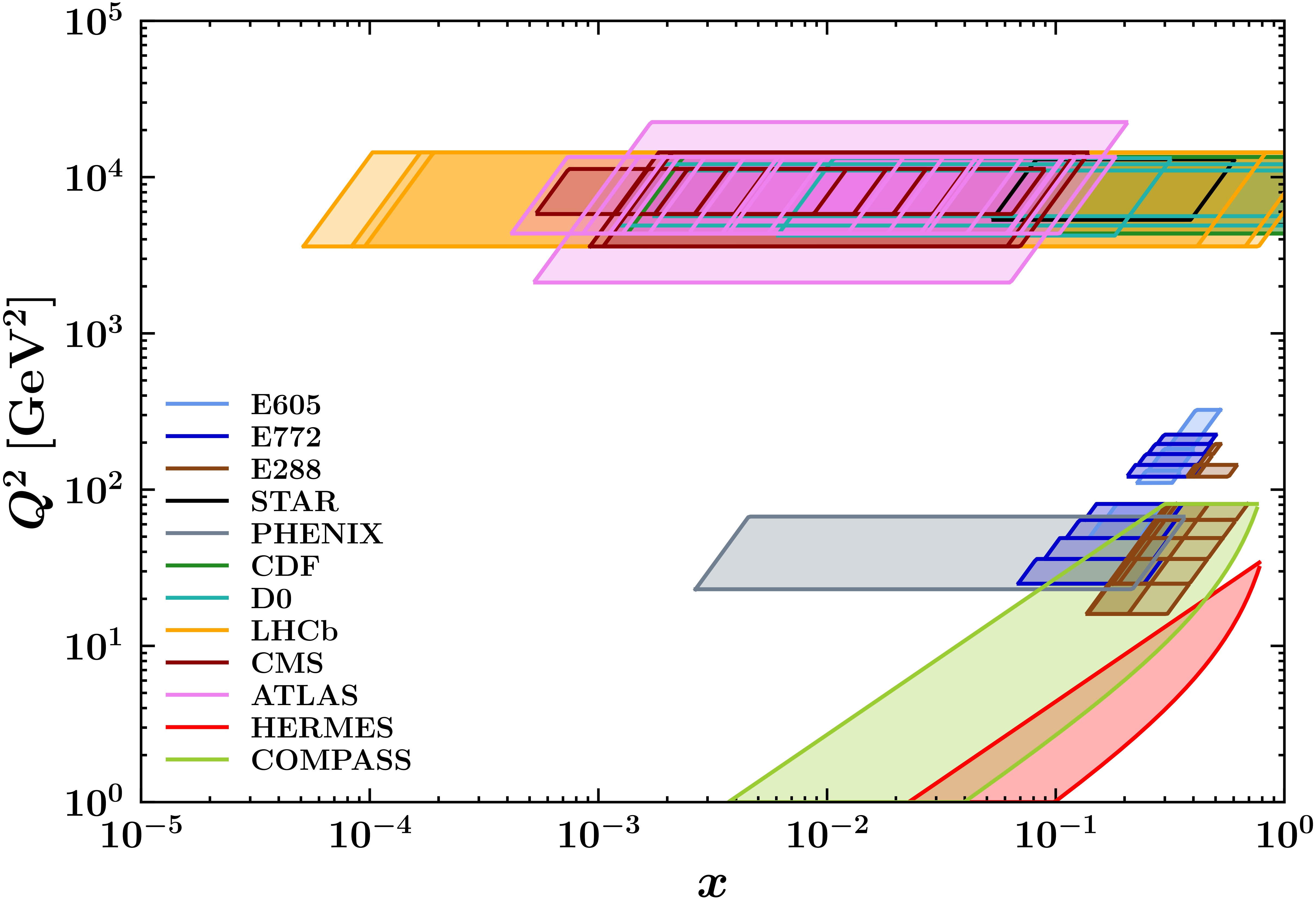

MAPTMD 2022

Fit quality

	N^3LL^-			
Data set	N_{dat}	χ^2_D	χ^2_λ	χ^2_0
CDF Run I	25	0.45	0.09	0.54
CDF Run II	26	0.995	0.004	1.0
D0 Run I	12	0.67	0.01	0.68
D0 Run II	5	0.89	0.21	1.10
D0 Run II (μ)	3	3.96	0.28	4.2
Tevatron total	71	0.87	0.06	0.93
LHCb 7 TeV	7	1.24	0.49	1.73
LHCb 8 TeV	7	0.78	0.36	1.14
LHCb 13 TeV	7	1.42	0.06	1.48
LHCb total	21	1.15	0.3	1.45
ATLAS 7 TeV	18	6.43	0.92	7.35
ATLAS 8 TeV	48	3.7	0.32	4.02
ATLAS 13 TeV	6	5.9	0.5	6.4
ATLAS total	72	4.56	0.48	5.05
CMS 7 TeV	4	2.21	0.10	2.31
CMS 8 TeV	4	1.938	0.001	1.94
CMS 13 TeV	70	0.36	0.02	0.37
CMS total	78	0.53	0.02	0.55
PHENIX 200	2	2.21	0.88	3.08
STAR 510	7	1.05	0.10	1.15
DY collider total	251	1.86	0.2	2.06

E288 200 GeV	30	0.35	0.19	0.54
E288 300 GeV	39	0.33	0.09	0.42
E288 400 GeV	61	0.5	0.11	0.61
E772	53	1.52	1.03	2.56
E605	50	1.26	0.44	1.7
DY fixed-target total	233	0.85	0.4	1.24
HERMES ($p \to \pi^+$)	45	0.86	0.42	1.28
HERMES ($p \to \pi^-$)	45	0.61	0.31	0.92
HERMES ($p \to K^+$)	45	0.49	0.04	0.53
HERMES ($p \to K^-$)	37	0.18	0.13	0.31
HERMES ($d \to \pi^+$)	41	0.68	0.45	1.13
HERMES ($d \to \pi^-$)	45	0.63	0.35	0.97
HERMES ($d \to K^+$)	45	0.2	0.02	0.22
HERMES ($d \to K^-$)	41	0.14	0.08	0.22
HERMES total	344	0.48	0.23	0.71
COMPASS ($d \to h^+$)	602	0.55	0.31	0.86
COMPASS ($d \to h^-$)	601	0.68	0.3	0.98
COMPASS total	1203	0.62	0.3	0.92
SIDIS total	1547	0.59	0.28	0.87
Total	**2031**	**0.77**	**0.29**	**1.06**

MAPTMD 2022

Correlation between fit parameters

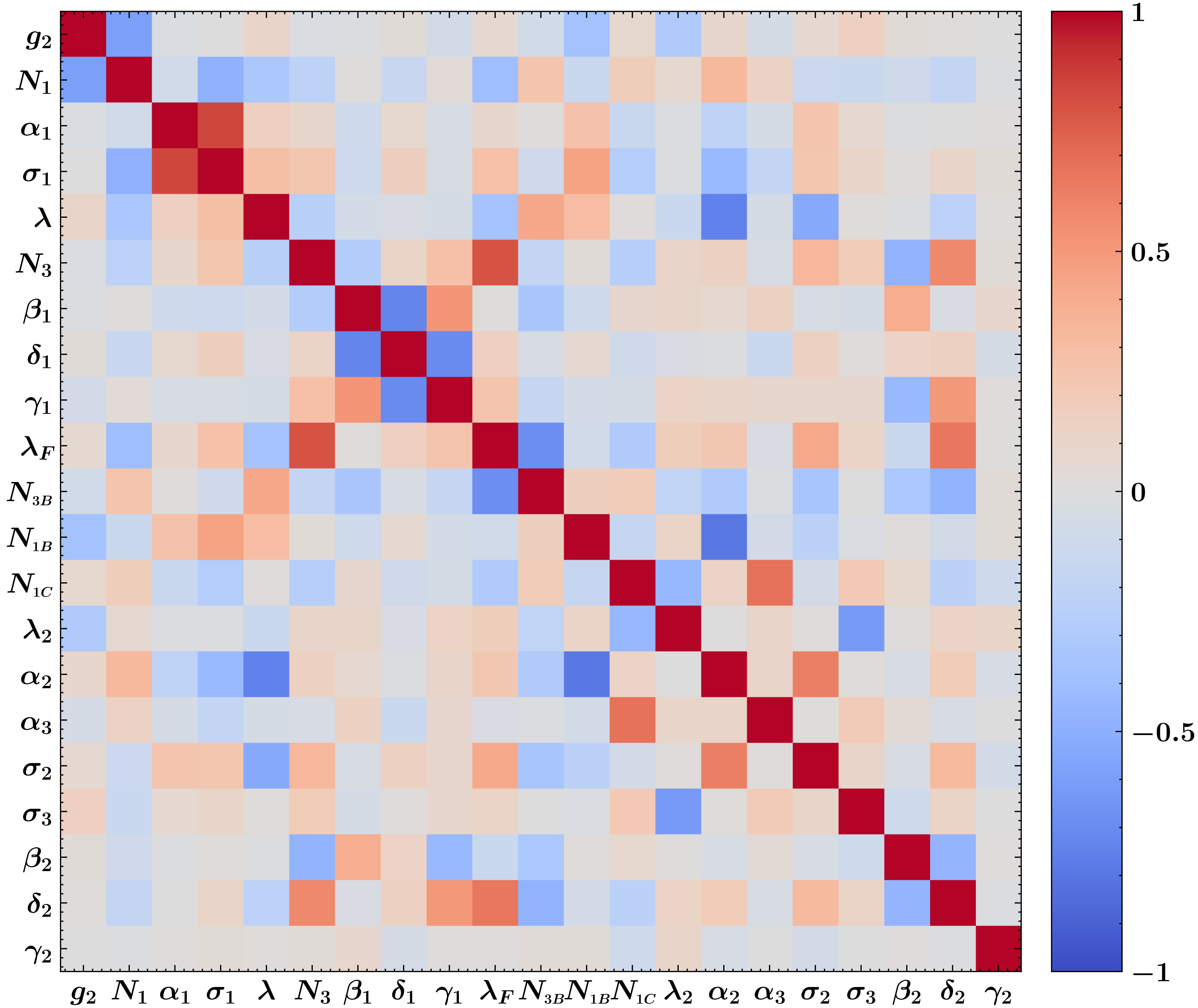

MAPTMD 2022

Fit quality: DY

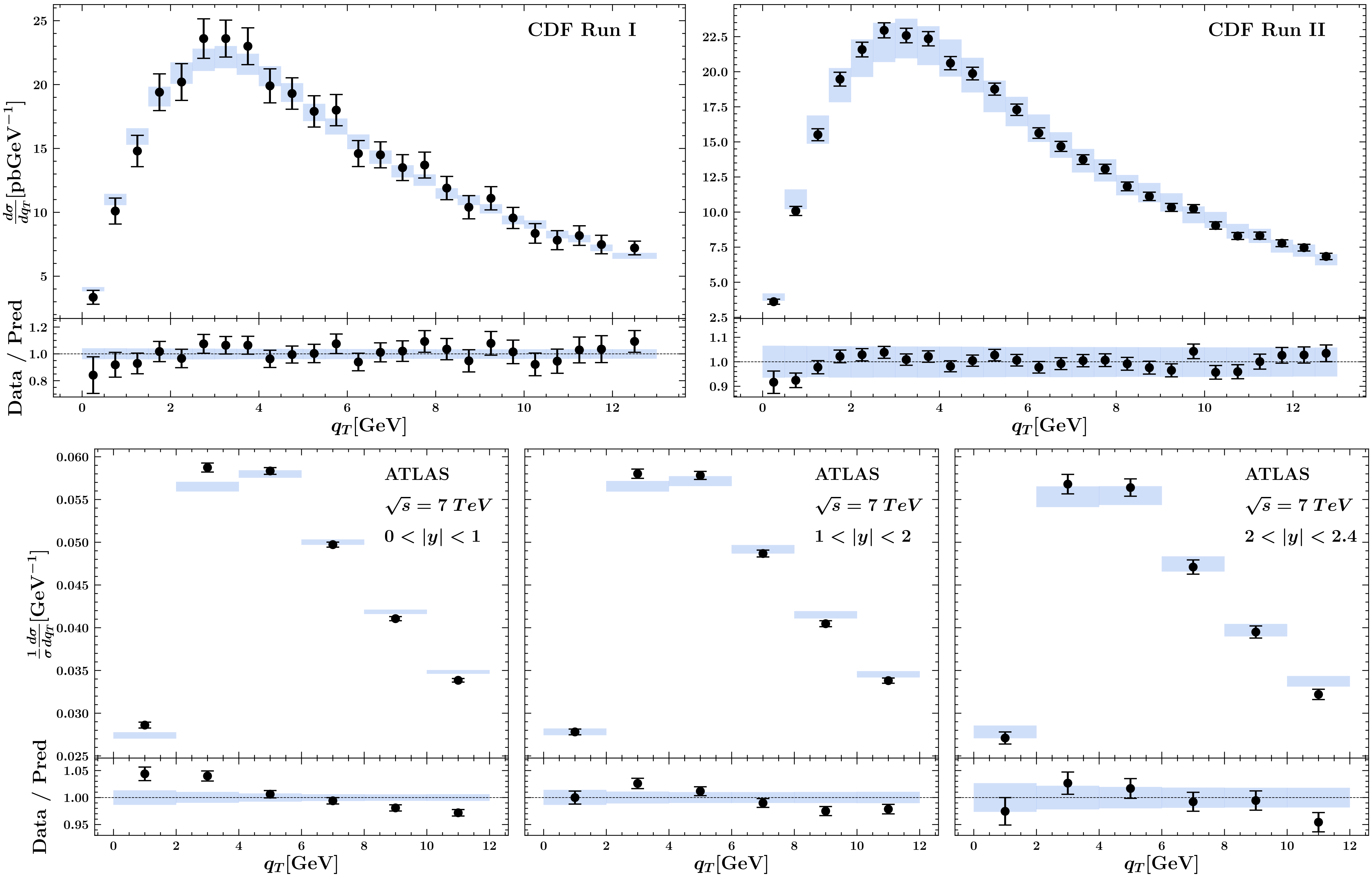

MAPTMD 2022

Fit quality: DY at LHCb

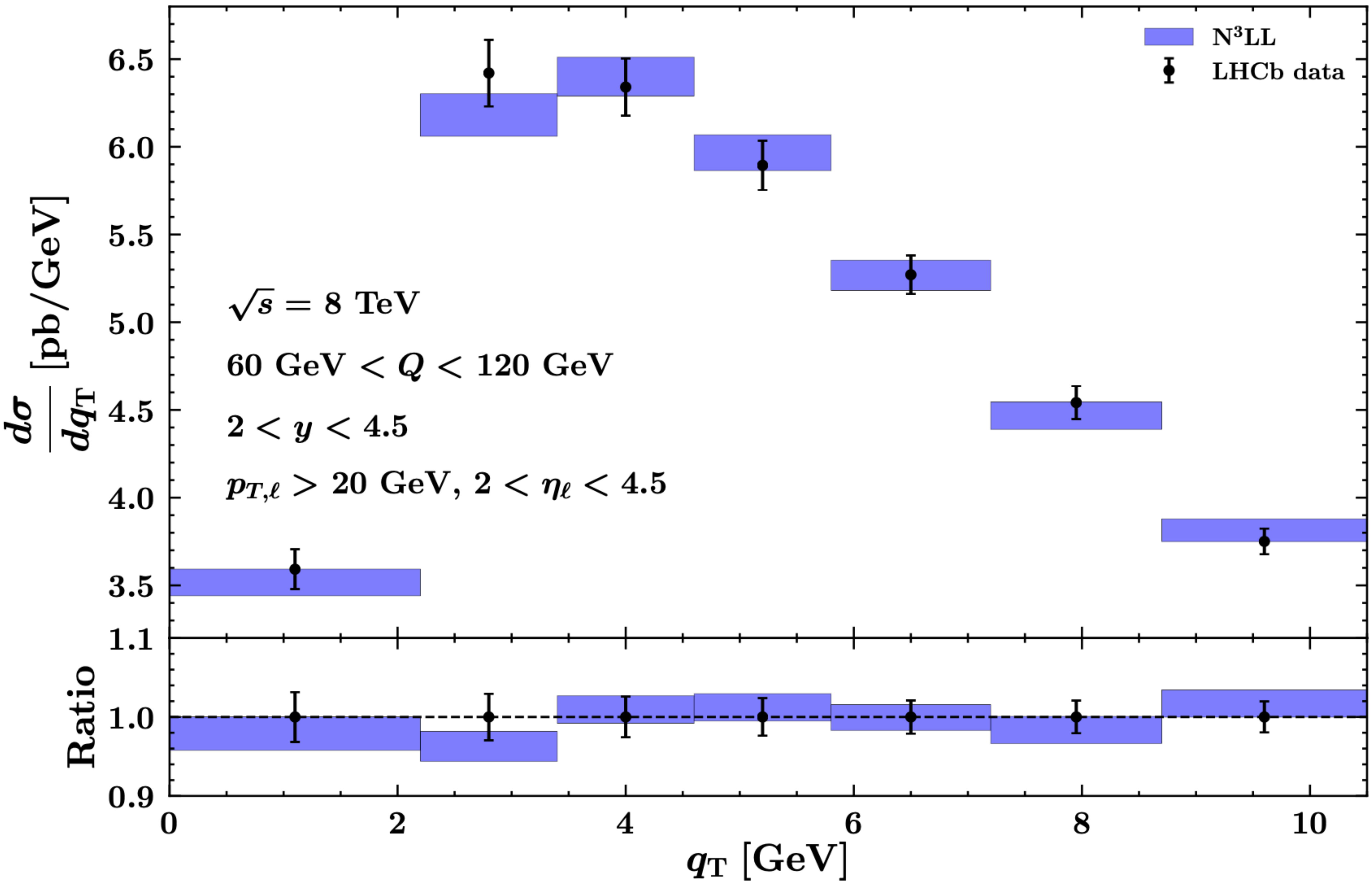

Perturbative convergence

	NLL′	NNLL	NNLL′	N^{3}LL
Global χ^2	1126	571	379	360

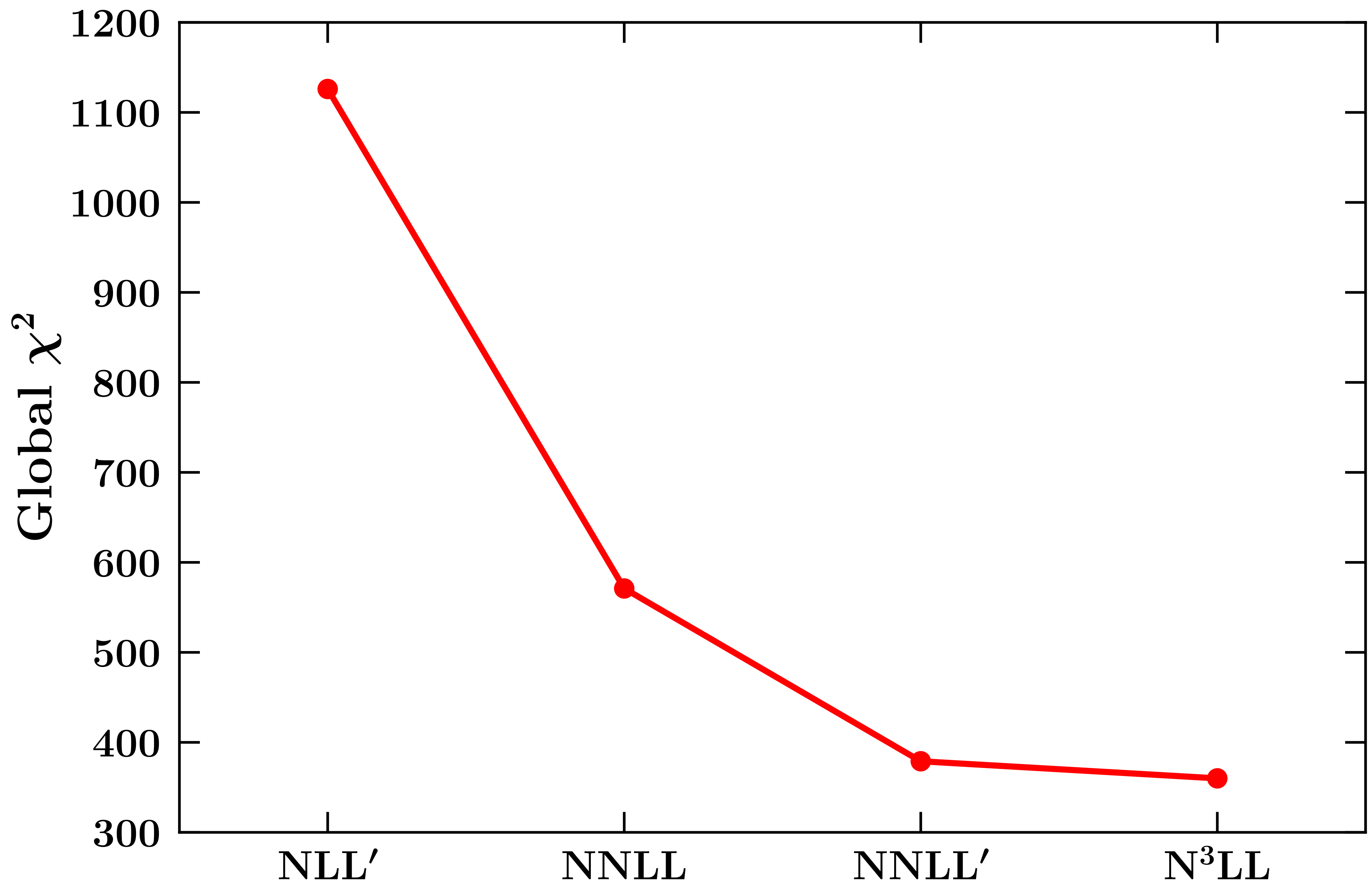

Perturbative convergence